



1

2 **The chemical characteristics of rainwater and wet atmospheric**
3 **deposition fluxes at two urban sites and one rural site in Côte d'Ivoire.**

4 **Mohamed L. Kassamba-Diaby¹, Corinne Galy-Lacaux², Veronique Yoboué¹, Jonathan E. Hickman**
5 **³, Kerneels Jaars⁴, Sylvain Gnamien¹, Richmond Konan¹, Eric Gardrat², Siele Silué⁵**

6 ¹Laboratoire des Sciences de la Matière, de l'environnement et de l'énergie Solaire / Université Félix
7 Houphouët-Boigny, Abidjan BPV 34, Côte d'Ivoire

8 ²Laboratoire d'Aérodologie, Université Toulouse III Paul Sabatier / CNRS, Toulouse, France

9 ³Center for Climate Systems Research, Columbia University, New York, USA

10 ⁴Atmospheric Chemistry Research Group, Research Focus Area: Chemical Resource Beneficiation,
11 North-West University, Potchefstroom, South Africa

12 ⁵University Peloforo Gbon Coulibaly/ Korhogo, Côte d'Ivoire

13 Corresponding author: Mohamed Lamine Kassamba Diaby, email: diabykassamba@yahoo.fr, Université
14 Felix Houphouet Boigny, address: 01 BP V 34, 01 Abidjan

15 Key words

16 Rainwater, chemical composition, wet deposition, acidification, neutralization, eutrophication

17 urban and rural sites, Cote d'Ivoire, Africa

18

19 Abstract

20 In this study, we characterized the chemical composition of precipitation at three sites in Côte d'Ivoire
21 representative of a south-north transect. Two urban sites have been selected in the framework of the
22 Pollution and Health in Urban Areas (PASMU) project: one located in Abidjan in the coastal climate zone
23 and the other located in Korhogo in the northern climate zone. The third site is the International Network to
24 study Deposition and Atmospheric chemistry in Africa (INDAAF) rural site of Lamto representative of a
25 wet savanna and located in the central climate zone. This work documents a three-year time period (2018-
26 2020) with 221 samples, 239 samples and 143 samples which have been collected in Abidjan, Lamto and
27 Korhogo, respectively. Annual and monthly VWM concentration of major ions (Na^+ , K^+ , Mg^{2+} , Ca^{2+} , Cl^- ,
28 NO_3^- , SO_4^{2-} , NH_4^+ , HCOO^- , CH_3COO^- , $\text{C}_2\text{H}_5\text{COO}^-$, $\text{C}_2\text{O}_4^{2-}$) in rainwater have been calculated and were found
29 to follow the following patterns: $\text{Ca}^{2+} > \text{Cl}^- > \text{Na}^+ > \text{NH}_4^+ > \text{SO}_4^{2-} > \text{Tcarb} > \text{NO}_3^- > \text{Mg}^{2+} > \text{HCOO}^- > \text{CH}_3\text{COO}^-$
30 $> \text{K}^+ > \text{H}^+ > \text{C}_2\text{O}_4^{2-} > \text{C}_2\text{H}_5\text{COO}^-$ in Abidjan, $\text{NH}_4^+ > \text{HCOO}^- > \text{Ca}^{2+} > \text{NO}_3^- > \text{CH}_3\text{COO}^- > \text{H}^+ > \text{Cl}^- > \text{Na}^+$



31 $\text{SO}_4^{2-} > \text{Mg}^{2+} > \text{K}^+ > \text{Tcarb} > \text{C}_2\text{O}_4^{2-} > \text{C}_2\text{H}_5\text{COO}^-$ in Lamto and $\text{Ca}^{2+} > \text{NH}_4^+ > \text{Na}^+ > \text{HCOO}^- > \text{NO}_3^- > \text{Cl}^-$
32 $> \text{K}^+ > \text{CH}_3\text{COO}^- > \text{SO}_4^{2-} > \text{H}^+ > \text{Mg}^{2+} > \text{Tcarb} > \text{C}_2\text{O}_4^{2-} > \text{C}_2\text{H}_5\text{COO}^-$ in Korhogo. The average pH values
33 are respectively 5.76, 5.31, 5.57 for Abidjan, Lamto and Korhogo with a preponderance of mineral acidity
34 at the urban sites representing respectively 69 % and 52% of the total acidity contribution in Abidjan and
35 Korhogo while the organic acidity is more important in Lamto representing 62 % of the total acidity
36 contribution. Dry seasons contribute to 46%, 74 % and 86% to the total measured chemical content of
37 precipitation respectively at Abidjan, Lamto and Korhogo. During dry seasons, Lamto and Korhogo rainfalls
38 are more impacted by biomass burning source and continental air mass loaded in terrigenous compounds
39 than Abidjan. Conversely, during wet seasons Abidjan rainfalls are more impacted by oceanic air mass from
40 guinean gulf rich in sea salt than Lamto and Korhogo.

41

42 1.Introduction

43 Atmospheric deposition represents a key mechanism in anthropogenic impacts on the environment.
44 Atmospheric deposition includes wet and dry processes, and is the major removal pathway of atmospheric
45 pollutants and thus contributes to the equilibrium of the earth-atmosphere biogeochemical balance (Vet et
46 al., 2014; Laouali et al., 2021; Fu et al., 2021; Galy-Lacaux et al., 2009). Limiting anthropogenic impacts
47 on atmospheric deposition is considered fundamental for addressing several sustainable development goals
48 such food security, climate change, human health and biodiversity (Rockström et al., 2009; Fowler et al.,
49 2013; Fu et al., 2021). The study of deposition processes and the determination of deposition fluxes is
50 important for understanding the spatial and temporal evolution of the chemical composition of the
51 atmosphere and of the biogeochemical cycles of elements such as nitrogen, carbon and sulfur. Where
52 biogeochemical cycles are strongly affected by anthropogenic activities, atmospheric deposition can act as
53 a source of nutrients but also as a source of toxins (Bobbink et al., 2010; Zhang et al., 2007a; Whelpdale et
54 al., 1997).

55 Wet deposition plays a key role in removing both gaseous and particulate pollutants from the atmosphere
56 and thus influences atmospheric chemistry (Seinfeld and Pandis, 1998; Laouali et al., 2012). Rain chemical
57 composition provides insights into the evolution of the chemical composition of the atmosphere, and is
58 influenced by numerous factors including the type and strength of natural/anthropogenic sources of
59 atmospheric compounds, long-range transport, the origin of continental air masses, as well as removal
60 processes related to the intensity and temporal distribution pattern of rainfall (Vet et al., 2014; Akpo et al.,
61 2015; Keresztesi et al., 2019). In addition, rainfall composition is useful for understanding direct impacts
62 on ecosystems and is an important indicator in the determination of the pollution levels in urban areas
63 (Moreda-Piñeiro et al. 2014; Martins et al. 2019; Gao et al. 2020; Günzel 2020). Lack of accurate
64 descriptions of deposition processes and thorough evaluation with high-quality measurements remain a
65 major weakness of global deposition modelling. This is particularly true in tropical regions, which are often



66 affected by convective rainfall regime, and where long-term high-quality data on deposition are scarce
67 (Fowler et al., 2013; Vet et al., 2014; Fu et al., 2021).

68 To date, the most recent study in this context is the global assessment of precipitation chemistry and
69 deposition carried out under the auspices of the World Meteorological Organization (WMO) -Global
70 Atmospheric Watch (GAW) Scientific Advisory Group Total Atmospheric Deposition (SAG TAD), which
71 aims to characterize precipitation chemical composition and to quantify deposition fluxes (wet, dry, total)
72 of sulfur, nitrogen, acidity, sea salt, organic acids and phosphorus at global and continental scales. The study
73 compares two temporal reference periods: 2000-2002 and -2005-2007 (Vet et al., 2014). The conclusion of
74 that assessment led to some recommendations to address major gaps and uncertainties in global ion
75 concentration and deposition measurements. One of these recommendations emphasizes the lack of
76 measurements in tropical regions and the weakness of the spatial coverage in different continents such as
77 South America, parts of India and Africa (Vet et al., 2014; Fu et al., 2021).

78 The assessment recognized the importance of the unique long-term quality-controlled database in Africa
79 provided by the International Network to study Deposition and Atmospheric chemistry in Africa (INDAAF,
80 <https://indaaf.obs-mip.fr>) even though the number of measurements stations remain low. The INDAAF
81 program, initiated in 1994, aims to study atmospheric composition and wet and dry deposition fluxes in
82 Africa. It is part of the Deposition of Biogeochemically important Trace Species (DEBITS) activity of the
83 International Global atmospheric Chemistry (IGAC) as well as an official contributor network to the
84 GAW/WMO program and a labeled component of the Aerosol Cloud and Trace gases Research
85 Infrastructure (ACTRIS).

86 The INDAAF activity is based on a regional long term monitoring network of 10 stations representative of
87 three major African ecosystems covering dry savanna, wet savanna and equatorial forest ([https://indaaf.obs-](https://indaaf.obs-mip.fr)
88 [mip.fr](https://indaaf.obs-mip.fr) (Laouali et al., 2021). High quality measurements of atmospheric chemistry (rainwater, aerosol and
89 gaseous chemical composition) are performed on a multi-year scale. Many synthesis studies which are
90 representative of ecosystem rural sites, or which rely on the comparison of the eco-systemic transect dry
91 savannas, wet savannas-forests, have been published (Laouali et al., 2012; Yoboué et al., 2005a; Akpo et
92 al., 2015; Galy-Lacaux et al., 2009; Galy-Lacaux and Modi, 1998). Although these works have characterized
93 precipitation chemistry and deposition in Africa representative of rural areas, there are no studies to our
94 knowledge that consider urban areas in Africa. In the context of the rapid urbanization and demographic
95 explosion in Africa (United Nations, Department of Economic and Social Affairs, Population Division
96 2017; Kaba et al. 2020), it is important to improve our understanding of urban areas precipitation
97 composition and the ion deposition fluxes at the seasonal and annual scale in order to assess the evolution
98 of atmospheric composition and the potential impacts of pollutants under the influence of increasing human
99 activity in cities and megacities in developing countries.



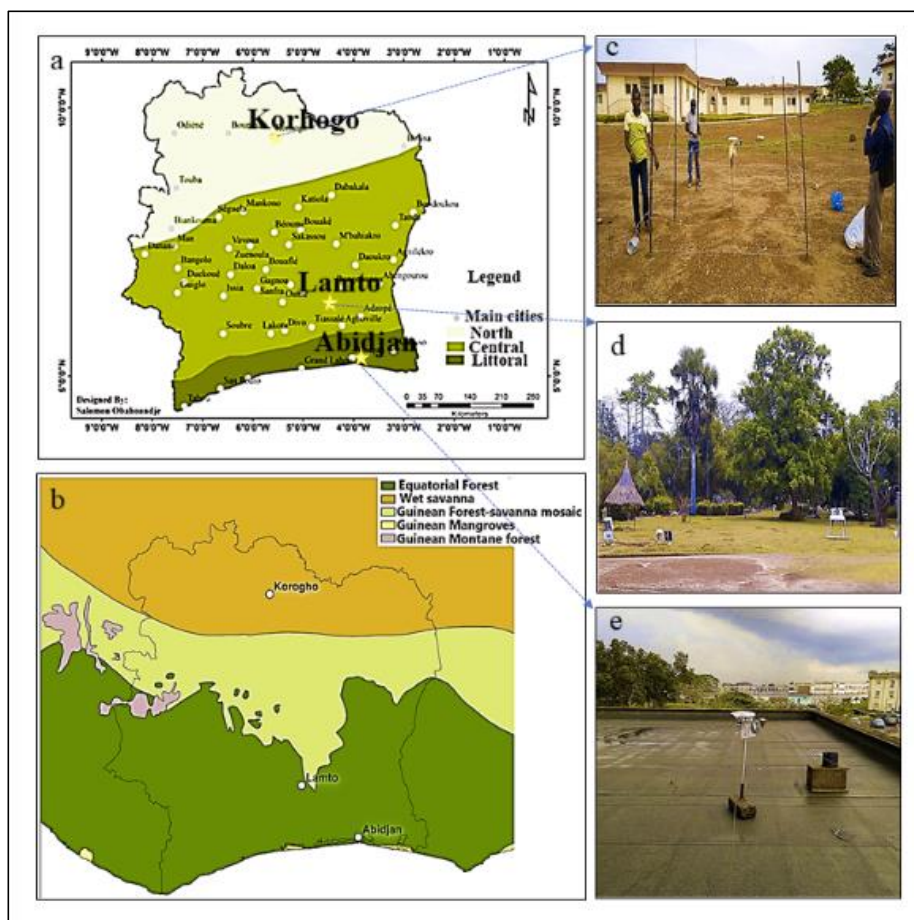
100 In Côte d'Ivoire, the percentage of the national population living in urban areas is expected to increase to
101 60% by 2025 and exceed 70% by 2050 (UN World Urban Population , 2011). Increased urbanization and
102 population will likely be accompanied by increasing pollutants emissions from fossil fuel consumption, as
103 in other countries such as in China which experienced extreme pollution levels following its fast economic
104 development (Wang et al., 2008; Zhang et al., 2007).

105 The present study proposes to investigate precipitation chemistry and wet deposition fluxes over a south
106 north transect in Côte d' Ivoire, considering three measurements sites, including two urban and one rural
107 site. This work is performed in collaboration with two major monitoring programs: the Air Pollution and
108 Health in Urban Areas (PASMU) implemented in 2018 to study the atmospheric chemical pollution and
109 impacts on human health in the economic capital of Côte d'Ivoire (Abidjan) and in the regional city of
110 Korhogo in relation to meteorological parameters and emission sources (Gnamien et al., 2021); and the
111 INDAAF program, which includes the site of Lamto, representative of a soudano-guinean wet savanna.

112 The main objective of the present study is to establish the characteristics of the chemical composition of
113 precipitation and the deposition fluxes of two urban areas and one rural area in Côte d' Ivoire, together
114 representative of a continental south-north transect. The goals of this study are: (1) to document over a three-
115 year time period (2018-2020) the rainwater chemical composition and the deposition fluxes of soluble ions,
116 including concentrations of major ions, the variation of pH, concentrations of sea salts, the neutralizing
117 capacity of precipitation, and ion enrichment factors, (2) to provide a better understanding of ion sources
118 and the climatology that influence annual, seasonal and monthly precipitation content and (3) to analyze the
119 intra-annual and seasonal variability of precipitation composition and associated wet deposition fluxes for
120 the different ionic species. This study offers a baseline record for urban sites in African cities against which
121 future changes in emissions and potential environmental impacts can be evaluated, and responds to
122 international recommendations that emphasize the scarcity of deposition measurements on the African
123 continent, recognized at a global scale to be a continent faced with major environmental sustainability issues
124 (World Bank, 2017; World Meteorological Organization, 2021).

125 2. Materials and Methods

126 2.1. Sites description



127

128 Figure 1: Locations of the three measurement sites on the Abidjan-Lamto-Korhogo transect: (a): map of climatic
129 subdivision in Côte d'Ivoire adapted from (Kouadio et al, 2007); (b): map of ecoregions subdivision in Côte
130 d'Ivoire (c): of Korhogo; (d): Lamto; (e): Abidjan.

131

132 This study considers three measurement sites, two urban and one rural, located along a south-north transect
133 in Côte d'Ivoire (Figure 1). The two urban sites, Abidjan and Korhogo, have been selected and studied in
134 the framework of the PASMU program, and are respectively located in the south and north of Côte d'Ivoire.
135 The modes of transportation, the types of fuel used by households and the population density make it
136 possible to distinguish and characterize both of these urban sites. It is worth noting that in Côte d'Ivoire,
137 southern cities are generally more populated and industrialized than those in the north. For example,
138 Abidjan's population is 10 times larger than that of Korhogo (Gnamien et al., 2021) and according to (Fall
139 et al., 2016), Ivorian cities can be divided into three categories : global connectors, which are cities such as
140 Abidjan, that generate the economies of urbanization necessary for innovation, increasing returns to scale
141 activities and global competitiveness; regional connectors, that are cities such as Korhogo, which generate



142 the local economies necessary for efficient regional trade and transportation, and local connectors, that are
143 cities that generate the economies of scale necessary to release agricultural potentials of their regions.

144 The first urban site is located in Abidjan (5° 20' 43." N; 4° 1' 27." W) which is a metropolitan area on the
145 south-east coast of Côte d'Ivoire and considered to be the economic capital of the country, Abidjan is the
146 largest city in Côte d'Ivoire with a population over 4 707 404 million, which is approximately 20 % of the
147 population in Côte d'Ivoire, and a surface area of 2119 km² (INS, 2014). This city is an autonomous district
148 divided in 13 suburbs. The sampling site was on the roof top of the Institut de Recherche et de Development
149 (IRD) building, which is in the suburb of Cocody, in the vicinity of the University Felix Houphouet Boigny.
150 The major pollution sources in the city are fossil fuel consumption from traffic of motorized vehicles,
151 household coal burning and emissions from industrials activities. (Yao et al., 2016) estimated that the
152 national fleet of vehicles was 636 551 in 2016 with 80% in Abidjan (498.531 vehicles).

153 The second urban site is located in the city of Korhogo (9° 28' N; 5° 36' 51" W), which is situated in the
154 north of Côte d'Ivoire, approximatively 635 km from Abidjan in the savannas district. Korhogo is spread
155 over an area of 12.50 km² and has a population of 243 048 inhabitants, according to the last population
156 census in 2014 (INS, 2014). Korhogo is strongly influenced by agricultural activities, even though it is an
157 urban area. According to Bassett et al. (2018), Korhogo is the epicenter of the cotton and cashew boom
158 culture, which is dependent on fertilizers and pesticides for crop production. In terms of the level of
159 urbanization and industrialization, Korhogo is far from the level of megacities such as Abidjan, although it
160 has recorded substantial population growth since the political crisis in 2002, resulting in the surface of the
161 city increasing from 3300 ha in 2000 ha to 10000 ha in 2019 (Sangare et al., 2021). Nonetheless, it has a
162 relatively low level of urbanization and industrialization compared to Abidjan. The mode of transport is
163 dominated by two-wheeled vehicles. This trend is also observed at the level of public transport with the
164 emergence of motorcycle cabs, Taxi-motos", which constitute one of the principal means of transport since
165 the prohibition of four-wheeled taxi vehicles at the time of the political-military crisis in September 2002
166 (Roger et al., 2016).

167 The third sampling site, Lamto, represents a super-site of the INDAAF project and is located in the central
168 part of the country, at the tip of the "V Baoule". Lamto (6°13' N, 5°02' W) is located in the region of Agnéby-
169 Tiassa, in the department of Tiassalé, about 165 km in the north-west of Abidjan and 433 km in the south-
170 east of Korhogo. It is in a natural reserve that covers approximately 2600 ha and is representative of a
171 soudano-guinean wet savanna with the so-called, gallery forest along the Bandama river (Gautier et
172 al.,1990).

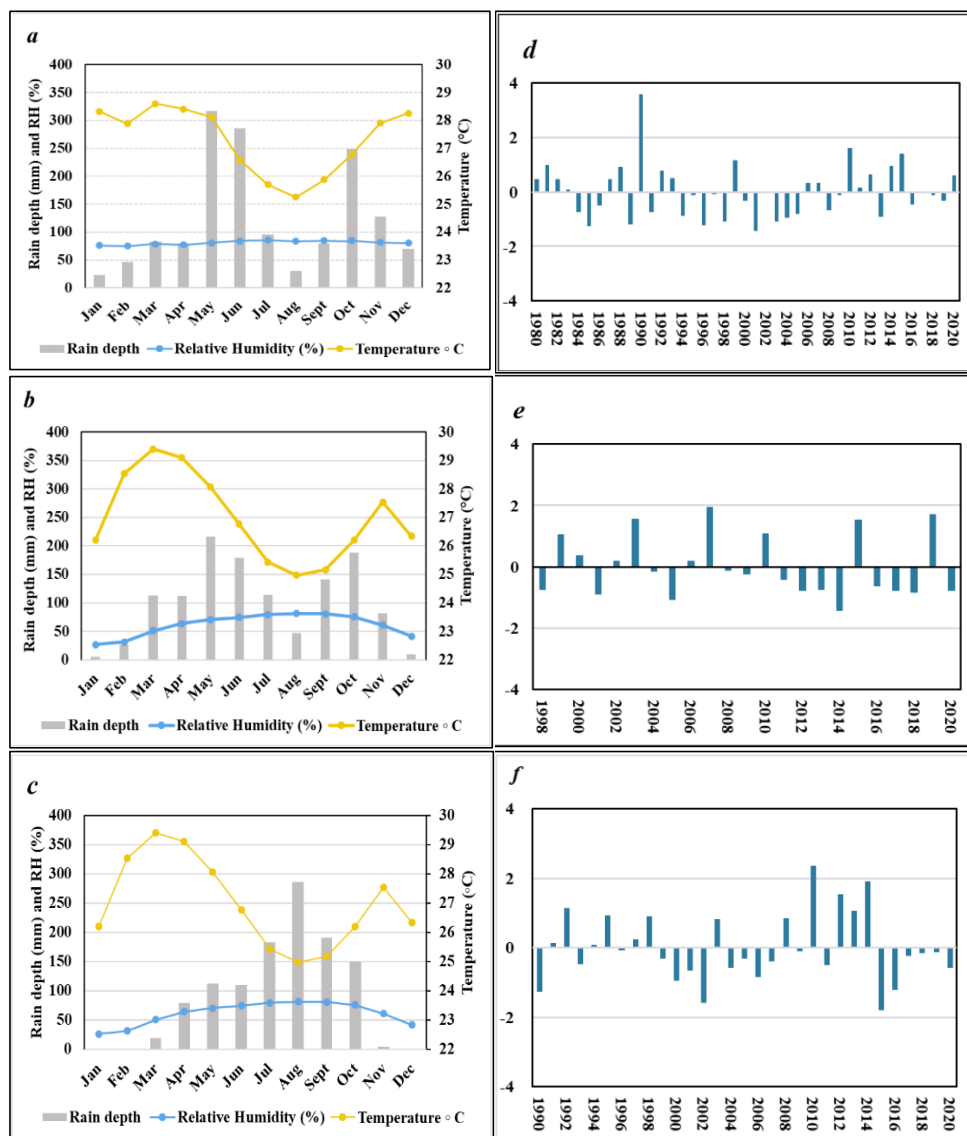
173 2.2. Climatology

174 West African climate depends on the position of the Intertropical zone of convergence (ITZC), which is the
175 limit between a cool and humid marine air mass (Monsoon) and a warm and dry Saharan air mass



176 (Harmattan). Climate is largely is influenced by the ITCZ variability at regional scale in Côte d' Ivoire.
177 Indeed, the extreme latitudinal positions of ITCZ zone in January (5°N) and in August (22°N) divide the
178 climate into three distinct zones: the Northern climatic zone, the Central climatic zone and the Coastal
179 Climatic zone (Kouadio et al., 2003) (Figure 1-a) . The three experimental sites are each situated in a
180 different zone: Abidjan in the Coastal Climatic zone, Lamto in the central climatic zone and Korhogo in the
181 Northern climatic zone. In These climatic zones , we have different pluviometric regimes: the tropical
182 regime of transition, the humid tropical regime of transition, the dimmed equatorial regime of transition, the
183 equatorial regime of transition and littoral equatorial regime of transition (Goula et al., 2010).
184 Meteorological parameters from 2018 to 2020 (monthly temperature and relative humidity) were provided
185 by the SODEXAM (Society of exploitation and airport development, Aeronautics and Meteorology) for
186 Abidjan and Korhogo, as well as long-term rainfall databases for the periods 1980-2020 and 1990-2020
187 respectively. From 2018 to 2020 in Abidjan, we used rainfall measured by the EVIDENCE project (Extreme
188 rainfall events, vulnerability to flooding and water contamination) that installed tipping bucket rain gauge
189 (tilting of the bucket for 0.5mm) and Précis Mécanique® (rain interception cone 1.5 m from the ground and
190 with an area equal to 400 cm²). Tipping bucket dates (day month year hour minute second) are recorded in
191 a HOBO Pendant® UA-003-64 data logger. The rain gauge data were collected monthly. During each visit,
192 the devices were cleaned and the tipping volume of the buckets was checked in the urban site of Abidjan.
193 At the Lamto site, the long-term monitoring program (INDAAF) provides air temperature, humidity and
194 rainfall data for the period (Diawara et al., 2014).

195
196
197
198
199
200
201
202
203
204
205
206
207
208
209
210



211

212 Figure 2: Monthly mean meteorological parameters measured at Abidjan (a), Lamto (b), and Korhogo (c)
 213 in 2019 (Air temperature (°C), Relative Humidity (%), Rain depth (mm)); Annual Inter variability Index
 214 (AII) for Abidjan (1980-2020) (d), Lamto (1998-2020) (e) and Korhogo (1990-2020) (f).

215

216

217

218

219

220



221 Abidjan is characterized by a bimodal rainfall regime defined by two wet seasons and two dry seasons. A
222 long-wet season lasts from March to July and a short-wet season from October to November. A long dry
223 season lasts from December to February and a short dry season from August to September (Leroux et al.
224 2001). Abidjan belongs to the coastal climatic zone characterized by a first rainfall maximum in June and a
225 second in September (Figure 2). The annual rainfall is in the range 784-3388.9 mm with an annual mean of
226 1522 ± 518 mm for the period 1980-2020. Lamto is situated in the central climatic zone, providing the site
227 with a mild climate warm and wet. We also distinguish two wet seasons and two dry seasons: one long wet
228 season that extends from March to July, mainly influenced by the monsoon air masses; one long dry season
229 from December to February, influenced by the Saharan air masses (harmattan) (Diawara et al., 2014); one
230 short dry season limited to the month of August; and one short wet season from September to November.
231 In terms of rainfall features, Lamto belongs to the equatorial coastal transition regime which has an annual
232 rainfall ranging from 991.9 to 1548.5 mm, with a mean annual rainfall of 1229 ± 165 mm for the period
233 1998-2020.

234 The Korhogo site is part of the north climatic zone, which is characterized by a unimodal rainfall regime,
235 varying between a single wet season from April to October and a single dry season from November to
236 March. Korhogo belongs to the tropical regime of transition, characterized by a maximum of rainfall in
237 August. The annual rainfall is between 867-1612 mm, with an annual mean of 1187 ± 179 mm from 1990
238 to 2020.

239 Observations in Abidjan show a weak fluctuation of air temperature and relative humidity during the studied
240 period (2018-2020). The annual mean temperature and relative humidity are approximately $27.30 \text{ °C} \pm 1.10$
241 and $80 \% \pm 3.89$ respectively (Figure 2). The maximum temperature is observed in March ($28.65 \pm 1.85 \text{ °C}$)
242 and minimum in August ($25.3 \pm 0.20 \text{ °C}$). Lamto meteorological parameters show a similar profile to
243 Abidjan. The maximum temperature is observed in February ($30.83 \pm 0.25 \text{ °C}$), followed by a gradual drop
244 until August, when the minimum temperature is observed ($26 \text{ °C} \pm 0.21$) (Figure 2). The mean relative
245 humidity over the study period is $77 \% \pm 5.53$. Air temperature and rainfall evolve in the opposite way.
246 During the gradual drop in temperature at the beginning of the year, we observe a gradual increase in
247 monthly rainfall (Figure 2). Korhogo presents a mean annual temperature and relative humidity of $27.00 \pm$
248 0.08 °C and $60 \% \pm 0.81$ respectively. Temperature increases from January to April to reach a monthly
249 maximum in April ($29.1 \pm 0.26 \text{ °C}$). The temperature then decreases gradually to a minimum in August
250 ($25.2 \pm 0.30 \text{ °C}$) that coincides with the beginning of the rainy season. The temperature then rises again until
251 november, followed by a sharp decrease in December.

252 Figure 2 presents also the calculation of the Annual Inter variability Index (AII) (Sarr, 2009), which enables
253 the characterization of the general patterns of precipitation over the study period. According to Sarr, the
254 degree of drought is a function of the index (AII) of precipitation. If $AII > 2$, the humidity is extreme, and

255



256 AII < - 2 represents extreme drought. The intermediate values of the index are classified as follows: 1 <
 257 AII < 2, 0 < AII < 1, - 1 < AII < 0 and - 2 < AII < - 1, corresponding to high humidity, moderate humidity,
 258 moderate drought and strong drought respectively. Considering data in Abidjan from 1980 to 2020, we have
 259 20 years of surplus and 18 years of deficit compared to an average rainfall of approximately 1522 mm, with
 260 the maximum rainfall recorded in 1990 (3338.9 mm) and the minimum in 2001 (784 mm). According to the
 261 classification of Sarr, 2020 (AII = + 0.14) can be considered as a moderately wet period while the other two
 262 years 2018 (AII = -0.08), 2019 (AII =-0.31) can be classified as moderately dry years. For Lamto, from
 263 1998 to 2020, there are 8 years of surplus and 13 years of deficit compared to an average rainfall of
 264 approximately 1229 mm. The maximum rainfall was recorded in 2007 (1548.5 mm) and the minimum in
 265 2014 (991.9 mm). For the three years of the study period, 2019 (AII =+1.7) can be considered as a strongly
 266 wet period while 2018 (AII =-0.8) and 2020 (AII =-0.8) can be classified as moderately dry years. Finally,
 267 at Korhogo from 1990 to 2020, we observe 12 years of surplus and 18 years of deficit with the respect to
 268 the average rainfall of 1187 mm. The maximum occurred in 2010 (1612 mm) and the minimum in 2015
 269 (866.7 mm). The three years of the study period, 2018-2020, are all years of deficit, with AII index values
 270 of -0.14, -0.15, -0.58 respectively. According to Sarr classification, they can be considered as moderately
 271 dry periods.

272 2.3. Sample collection

Sites	ABIDJAN			LAMTO			KORHOGO		
Year	2018	2019	2020	2018	2019	2020	2018	2019	2020
Pt (mm)	1477.7	1355.4	1593.7	1090.9	1508.2	1101.4	1160.7	1162.5	1083
Inter annual Variability (%)	-2.91	-10.94	4.71	-0.80	22.71	-10.38	-2.21	-2.06	-8.76
Pc (mm) Nc	825 (56)	1006.20 (81)	1288.30 (84)	1077.60 (91)	1459.40 (70)	988 (78)	745.55 (48)	862.80 (52)	783.10 (43)
% TP (%)	56	74	81	99	97	90	64	74	72
% PCL Annually % (quarterly)	75 (0,1,1,1)	100 (1,1,1,1)	100 (1,1,1,1)	100 (1,1,1,1)	100 (1,1,1,1)	100 (1,1,1,1)	75 (0,1,1,1)	100 (1,1,1,1)	100 (1,1,1,1)

273
 274 Table 1: Rainwater collection at Abidjan, Lamto and Korhogo (2018-2020): Annual Total Precipitation (Pt, mm),
 275 Interannual variability (%), Collected precipitation (Pc, mm) and Number of collected rain events (Nc), Percent total
 276 precipitation (%TP), Annual percent coverage length (%PCL) and in brackets: %PCL for each quarter (0 and 1 means
 277 0% and 100% respectively).

278
 279
 280
 281
 282



283 Precipitation sampling at the three sites was performed using a semi-automatic collector of precipitation
284 designed for the INDAAF (International Network to study Deposition and Atmospheric composition in
285 Africa) network (<http://indaaf.obs-mip.fr>). The equipment characteristics as well as the sampling protocols
286 have been fully described in several studies (Galy-Lacaux et al., 2009; Laouali et al., 2012; Akpo et al.,
287 2015). In brief, an automatic precipitation sampler made of up a single-use polyethylene bag, avoiding
288 aerosol deposit before the onset of the rain and a precipitation sensor automatically controls the aperture of
289 the sampler cover, which hermetically closes the polyethylene bag. At each site, a local technician collected
290 each rain event in a 50 mL Greiner tube, that was immediately placed in an on-site freezer (-18°C). The rain
291 sampling protocol follows the WMO/GAW international standards recommendations (WMO, 2004). After
292 collection, samples were sent for analysis at the Laboratoire d'Aerologie (Laero) in Toulouse, observing
293 very strict temperature regulation during the voyage. Table 1 presents the annual total precipitation (Pt) in
294 mm, the percent total precipitation (%TP) and the interannual variability as a percentage relative to the mean
295 annual rainfall for the 1980-2020 period, 1998-2020 period and 1990 -2020 period respectively for Abidjan,
296 Lamto and Korhogo. As defined by (WMO, 2004), (%TP) is the ratio between the annual precipitation (Pt)
297 and the collected precipitation (Pc). The annual and quarterly Percent Coverage Length (%PCL) which is
298 the percent of the summary period (e.g., month, season, year) for which information is available on whether
299 precipitation occurred or not is also indicated in Table 1. From April 2018 to December 2020 in Abidjan,
300 the total rainfall amount was 4426.8 mm and the collected rain samples represent a total of 3119.50 mm
301 with 221 samples. For Lamto, from January 2018 to December 2020 the total rainfall amount was 3700.5
302 mm and the collected rain samples represent a total rainfall amount of 3525 mm with 239 samples. For
303 Korhogo, from May 2018 to December 2020, the total rainfall was 3406.2 mm and the collected rain samples
304 represent a total of 2391.45 mm with 143 samples.

305 The %TP shows that rainwater collection in 2018 was not a good indicator of actual rainfall in Abidjan and
306 Korhogo, with values of 56 % and 64 % respectively. Lamto has good %TP values for all years. However,
307 for comparison purposes, only 2019 and 2020 will be considered for computing the annual volume weighed
308 mean (VWM) and Wet deposition fluxes (WD), and the average of the two years 2019-2020, where the
309 mean collection rate is respectively 78 %, 94 %, 73 % and the PCL is 100% in Abidjan, Lamto and Korhogo.
310 Data from January 2018 to December 2020 will be used to calculate monthly Volume Weighed Mean
311 (VWM) and Wet Deposition (WD) according to the quarterly %PCL. In reference to the WMO international
312 standards, we assume the precipitation collection at Abidjan, Lamto and Korhogo in 2019 and 2020 can be
313 considered as representative of the studied period according to the parameters calculated in Table 1.

314
315
316
317
318



319 2.4. Analytical procedures and quality assurance / quality control

320

321 Major inorganic (Na^+ , K^+ , Mg^{2+} , Ca^{2+} , Cl^- , NO_3^- , SO_4^{2-} , NH_4^+) and organic (HCOO^- , CH_3COO^- , $\text{C}_2\text{H}_5\text{COO}^-$,
322 $\text{C}_2\text{O}_4^{2-}$) ions were determined by Ionic Chromatography (IC) at Laero as described in (Galy-Lacaux and
323 Modi, 1998; Akpo et al., 2015). The Ionic chromatographic analysis is performed using a Thermo
324 ICS5000+ and an ICS 1100 Ionic chromatographs with two automated samplers (AS50). The eluents for
325 anions and cations are NaOH and MSA, respectively. Certified ionic standards are used for IC calibration.
326 pH is measured with an ATI Orion 350 instrument with a combined electrode (ATI Orion model 9252)
327 filled with KCl (4 M) and saturated with AgCl. Two standard solutions (WTW) at pH 4.01 and 7.00 are
328 used for its calibration. The precision is 0.01pH unit.

329 Since 1996, the Laboratoire d'Aerologie has participated to the bi-annual inter-laboratory comparison study
330 (LIS) of WMO-GAW precipitation quality assurance program. Results are available under the reference
331 700106 at the following address: <http://qasac-americas.org/>. According to these WMO inter-comparison
332 tests, analytical precision is 5% or better for all ions, within the uncertainties on all measured ionic values
333 presented here. Data quality is further ensured by calculating the ion difference for each sample to consider
334 the ionic balance (WMO, 2004). Analyses were performed on 221 rain samples collected in Abidjan, 239
335 rains samples collected in Lamto and 143 rains samples collected in Korhogo (Table 1). Results indicate in
336 Abidjan, Lamto and Korhogo respectively 208 or 94 % of collected samples, 236 or 98 % of collected
337 samples and 127 or 89 % are in the WMO acceptance range and will be considered in all the calculations
338 presented in the result sections.

339

340 2.5 Satellite data

341 We used version 1.6 of the CrIS-Fast Physical Retrieval (CFPR)- NH_3 product (Shephard et al. 2015; Mark
342 W. Shephard et al. 2020). CFPR is a physical retrieval of an atmospheric profile of NH_3 derived from
343 minimizing residuals between the measured and simulated spectra. The product compares well with in situ
344 and ground-based FTIR observations (Dammers et al., 2017; Kharol et al., 2018). The CrIS sensor has an
345 NH_3 detection limit of ~ 0.3 to 0.9 ppb (Shephard et al., 2020), which varies depending on the atmospheric
346 conditions. Comparing the NASA/NOAA SNPP satellite radiances from both CrIS and VIIRS instruments
347 show that the stability of CrIS is very good. The VIIRS – CrIS daily mean brightness temperature difference
348 shows a trend of -0.40 ± 0.03 mK per year at the wavelength of 10.76 μm for a ~ 273 K average scene (David
349 Tobin, personal communication). The most recent update of the CFPR (v1.6) identifies and accounts for
350 non-detect values below the sensor's detection limit, which reduces the previously reported small positive
351 bias for the lower range of total column concentrations ($< 5 \times 10^{15}$ molecules cm^{-2}). For this study, only



352 daytime observations from 2018 to 2020 are used. Note that observations for April-July 2019 are not
353 available, due to instrument error.

354 We used Level 3 (L3) data at 0.25°×0.25°resolution from the NASA tropospheric NO₂ standard product
355 from the Ozone Monitoring Instrument (OMI) aboard NASA's Aura satellite. OMI is a nadir-viewing
356 spectrometer in sun-synchronous orbit with near-daily global coverage that measures solar backscatter in
357 the UV-visible range (Krotkov et al., 2017). The OMI product relies on air mass factors calculated with the
358 assistance of an atmospheric chemical transport model, and is sensitive to model representations of
359 emission, chemistry and transport data. These are generally poorly constrained for regions not commonly
360 analyzed in chemical transport models such as sub-Saharan Africa region (McLinden et al., 2014). The L3
361 product includes only pixels that are at least 70% cloud-free, which may introduce additional bias: since the
362 product relies on nearly cloud-free retrievals, greater sunlight may induce higher photochemical rates. The
363 Level 2 OMI-NO₂ product has shown good agreement with in situ and surface-based observations (Lamsal
364 et al., 2014). For our analyses of satellite retrievals over Abidjan, Lamto and Korhogo, we selected
365 observations centered around the 0.25° grid cell containing each site to create a 1° field of NO₂ or NH₃
366 VCDs. The mean of this 1° grid cell was used as an estimate of VCDs over the site.

367 2.6. Calculations and statistics

368 The monthly Volume Weighed Mean (VWM) concentrations as well as the annual VWM concentrations in
369 $\mu\text{eq}\cdot\text{L}^{-1}$ for each ion were calculated using methods described by (Laouali et al., 2012; Conradie et al., 2016)
370 :

$$371 \quad \text{VWM} = \frac{\sum_{i=1}^N C_i \cdot P_i}{\sum_{i=1}^N P_i} \quad (1)$$

372 Where C_i in $\mu\text{eq}\cdot\text{L}^{-1}$ is the concentration of a given chemical element for each rain event, P_i is rainfall depth
373 for each rain event in mm. N is the number of rain events.

374 The annual as well as monthly wet deposition fluxes for all ionic species is expressed in $\text{kg}\cdot\text{ha}^{-1}\cdot\text{yr}^{-1}$ and
375 calculated by these following formulae (Laouali et al., 2021):

$$376 \quad \text{WD} = (\text{VWM} / c_i) * M_i * P_t / 100000 \quad (2)$$

377 Where VWM is the concentration in $\mu\text{eq}\cdot\text{L}^{-1}$, c_i is the ionic charge, M_i in $\text{g}\cdot\text{mol}^{-1}$ is the molar mass of each
378 species and P_t in mm is the annual rain depth for annual wet deposition fluxes and monthly rain depth for
379 monthly wet deposition fluxes.

380 The H^+ concentrations were calculated from measured pH values: $10^{-\text{pH}}$ (3)



381 Sea Salt Fraction (SSF) to ionic concentrations in rainwater and corresponding enrichment factors (EF) were
382 calculated according to the method suggested by many authors (Chao and Wong, 2002; Keene and
383 Galloway, 1986).

$$384 \quad EF_{\text{marine}} = [X/Na^+]_{\text{rain}} / [X/Na^+]_{\text{sea}} \quad (4)$$

$$385 \quad EF_{\text{crystal}} = [X/Ca^{2+}]_{\text{rain}} / [X/Ca^{2+}]_{\text{crystal}} \quad (5)$$

386 Where X is the concentration of the ion of interest, Na^+ is used as the element of reference for marine source
387 (Kulshrestha et al., 2003) and Ca^{2+} is selected as reference element for continental origin (Safai et al., 2004).

$$388 \quad SSF(X) = (X/[Na^+]_{\text{sea}}) * [Na^+]_{\text{rain}} \quad (6)$$

$$389 \quad NSS(X) = [X]_{\text{rain}} - SSF(X) \quad (7)$$

390 Where $SSF(X)$ is the marine part of the chemical element X in $\mu\text{eq.L}^{-1}$, $[Na^+]_{\text{rain}}$ is the concentration of Na^+
391 in rain ($\mu\text{eq L}^{-1}$) and $[X]/[Na]_{\text{sea}}$ is the ratio of species X to Na^+ in seawater (Keene et al., 1986). $NSS(X)$

392 is the non-marine part of the chemical element X in $\mu\text{eq L}^{-1}$ and $[X]_{\text{rain}}$ is the specific concentration of the
393 different species X in $\mu\text{eq. L}^{-1}$, the potential Acidity (pA) is defined as the sum of nitrate, sulfate, formic,
394 acetic, propionic and oxalic VWM concentrations, supposing that all ions are associated with H^+ .
395 $pA = \sum \text{anions} = [SO_4^{2-}] + [NO_3^-] + [HCOO^-] + [CH_3COO^-] + [C_2H_5COO^-] + [C_2O_4^{2-}] \quad (8)$

396 Fractional Acidity (FA); (Balasubramanian et al., 2001; Cao et al., 2009 ; Lu et al., 2011) is :

$$397 \quad FA = \frac{[H^+]}{([NO_3^-] + [SO_4^{2-}] + [HCOO^-] + [CH_3COO^-] + [C_2H_5COO^-] + [C_2O_4^{2-}])} \quad (9)$$

398 The Neutralization Factor (NF) (Celle-Jeanton et al., 2009; Rastogi and Sarin, 2005) is:

$$399 \quad NF_{xi} = \frac{[xi]}{([NO_3^-] + [SO_4^{2-}] + [HCOO^-] + [CH_3COO^-] + [C_2H_5COO^-] + [C_2O_4^{2-}])} \quad (10)$$

400 Where x_i are cations of interest, and all ionic concentrations are expressed in $\mu\text{eq L}^{-1}$.

401 The difference between neutralization potential (NP) ($Ca^{2+} + NH_4^+$) and acidic potential (AP) ($SO_4^{2-} + NO_3^-$)
402) is computing according to the following equation from (Safai et al., 2004): $NP/AP = [Ca^{2+}] + [NH_4^+] /$
403 $[SO_4^{2-}] + [NO_3^-] \quad (11)$

404 For study purposes, we adapted equations 8, 9, 10 and 11 by integrating the organic acidity which was not
405 included in the original equations used by the authors in previous studies. This approach enables us to take
406 into account all the acidity generated on the rainfall sampling sites.

407



408 2.7. Back trajectories

409 In order to determine the impact of air masses on the chemical composition of collected rainwater samples,
410 The air mass trajectories history for each site for the entire sampling period was determined by calculating
411 back trajectories with the Hybrid Single-Particle Lagrangian Integrated Trajectory (HYSPPLIT) model
412 (version 4.8), developed by the National Oceanic and Atmospheric Administration (NOAA) Air Resources
413 Laboratory (ARL) (Draxler and Hess, 1997). The model calculation method is a hybrid between the
414 Lagrangian approach, using a moving frame of reference for the advection and diffusion calculations as the
415 trajectories or air parcels move from their initial location, and the Eulerian methodology, which uses a fixed
416 three-dimensional grid as a frame of reference to compute pollutant air concentrations (The model's name,
417 no longer meant as an acronym, originally reflected this hybrid computational approach). Hourly-arriving
418 96-hour back trajectories were calculated at three arrival heights, 100, 1500 and 2500 m respectively, above
419 ground level. These individual back trajectories were then superimposed, in order to generate monthly or
420 seasonal overlay back trajectories for the study period, on a frequency map with a $0.2^\circ \times 0.2^\circ$ resolution grid
421 to show the statistical distribution. The frequency map has a color index that indicates the frequency of the
422 trajectories passing over the map grid cells. A color scale indicates the number of back trajectories passing
423 over a grid cell, with dark red indicating the highest percentage of back trajectory overpasses. All calculated
424 trajectories were visualized using MATLAB R2020b (<https://www.mathworks.com/>). The trajectories are
425 constructed using three-dimensional velocity fields, thereby making it an ideal method to incorporate
426 convective motions and the role thereof in the vertical transport of air masses (L Kok et al., 2021).

427 3. Results and discussion

428 3.1. Chemical composition of rainwater and wet deposition fluxes

429

430 Annual Volume Weighed Mean (VWM) concentrations and wet deposition fluxes (WD) computed for the
431 two-year sampling (2019-2020) along the South-North transect Abidjan-Lamto-Korhogo are presented in
432 the Table A1. At Abidjan, the chemical signature of the rainwater is characterized by the following ions
433 concentrations in decreasing order: $\text{Ca}^{2+} > \text{Cl}^- > \text{Na}^+ > \text{NH}_4^+ > \text{SO}_4^{2-} > \text{Tcarb} > \text{NO}_3^- > \text{Mg}^{2+} > \text{HCOO}^- >$
434 $\text{CH}_3\text{COO}^- > \text{K}^+ > \text{H}^+ > \text{C}_2\text{O}_4^{2-} > \text{C}_2\text{H}_3\text{COO}^-$. Ca^{2+} , Na^+ , Cl^- and NH_4^+ dominate and represent 62 % of the
435 rainwater total VWM ionic concentrations. At Lamto, the rainwater chemical signature is dominated by the
436 four following ions: NH_4^+ , HCOO^- , Ca^{2+} , and NO_3^- , representing 55 % of the total VWM ionic
437 concentrations. VWM concentrations follow a global pattern in the decreasing concentration order: $\text{NH}_4^+ >$
438 $\text{HCOO}^- > \text{Ca}^{2+} > \text{NO}_3^- > \text{CH}_3\text{COO}^- > \text{H}^+ > \text{Cl}^- > \text{Na}^+ > \text{SO}_4^{2-} > \text{Mg}^{2+} > \text{K}^+ > \text{Tcarb} > \text{C}_2\text{O}_4^{2-} > \text{C}_2\text{H}_3\text{COO}^-$.
439 Korhogo rainwater chemistry composition exhibits a profile dominated by the following ions Ca^{2+} , NH_4^+ ,
440 Na^+ , and HCOO^- , representing 53% of the total VWM ionic concentrations. The general chemical pattern
441 in the decreasing concentration order is: $\text{Ca}^{2+} > \text{NH}_4^+ > \text{Na}^+ > \text{HCOO}^- > \text{NO}_3^- > \text{Cl}^- > \text{K}^+ > \text{CH}_3\text{COO}^- >$



442 $\text{SO}_4^{2-} > \text{H}^+ > \text{Mg}^{2+} > \text{Tcarb} > \text{C}_2\text{O}_4^{2-} > \text{C}_2\text{H}_3\text{COO}^-$. The mean annual ionic load is estimated to 191.20 $\mu\text{eq.}$
 443 L^{-1} , 84.26 $\mu\text{eq. L}^{-1}$, and 111.75 $\mu\text{eq. L}^{-1}$ for Abidjan, Lamto and Korhogo respectively, demonstrating that
 444 the urban precipitations of Abidjan and Korhogo are much more loaded with ions than the rural area of
 445 Lamto.

446

447 3.1.1. Marine contribution

448 Sea-salt fractions (SSF), non-sea-salt fractions (NSSF) and enrichment factors (EF) for K^+ , Cl^- , Mg^{2+} , SO_4^{2-} ,
 449 Ca^{2+} ions were calculated according to the methodology outlined in section 2.5 (Table 2).

450

Sites	Sea water ratios (Keene et al, 1986)	Cl^-/Na^+	$\text{SO}_4^{2-}/\text{Na}^+$	K^+/Na^+	$\text{Ca}^{2+}/\text{Na}^+$	$\text{Mg}^{2+}/\text{Na}^+$
		1.167	0.121	0.022	0.044	0.227
ABIDJAN	Ratios in rain	1.23	0.75	0.17	1.47	0.28
	$\text{EF}_{\text{MARINE}}$	1	6	8	33	1
	SSF (%)	94	15	13	3	81
LAMTO	Ratios in rain	1.07	0.88	0.37	1.83	0.47
	$\text{EF}_{\text{MARINE}}$	1	7	17	42	2
	SSF (%)	92	10	5	2	35
KORHOGO	Ratios in rain	0.85	0.47	0.77	1.79	0.3
	$\text{EF}_{\text{MARINE}}$	1	1	35	41	1
	SSF (%)	100	16	3	2	75

451

452 Table 2: Seawater Enrichment Factor (EF) in Abidjan, Lamto and Korhogo

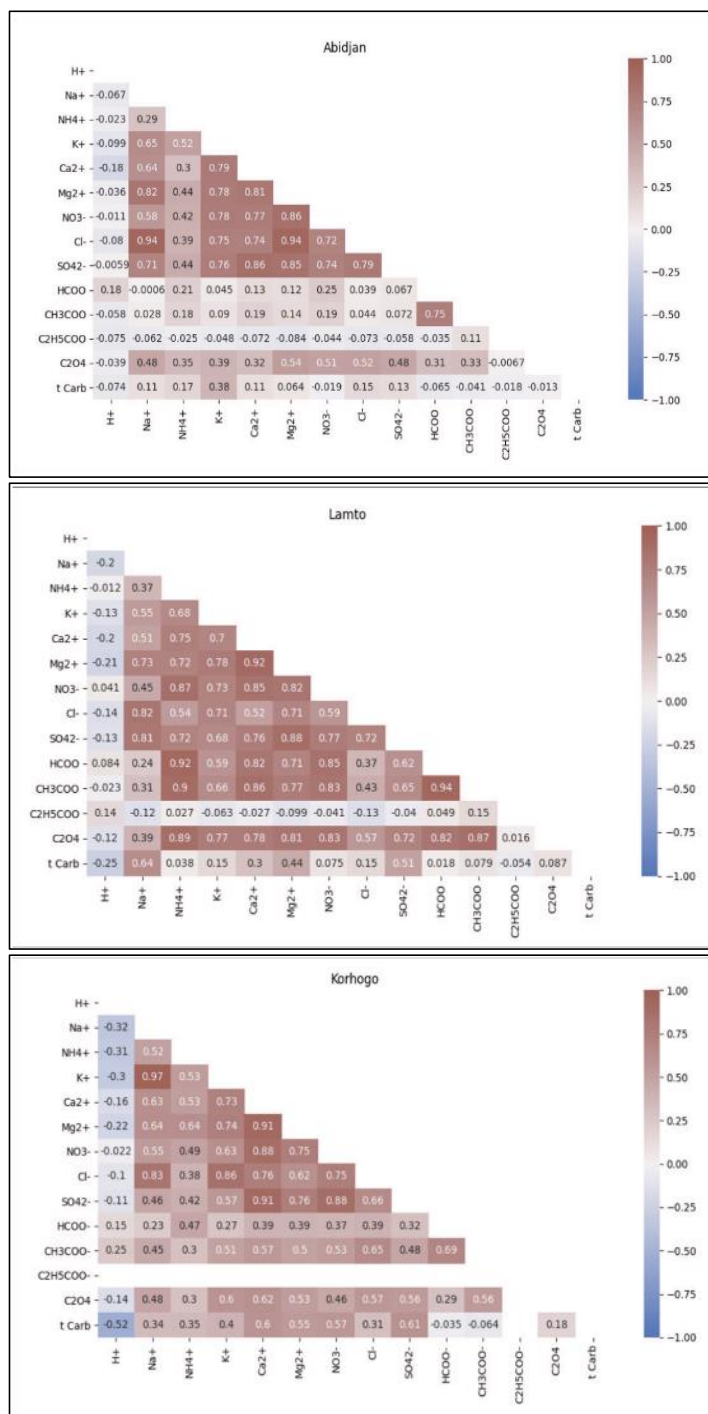
453 For the three studied sites, the Cl^-/Na^+ ratios were close to the sea-salt ratio of reference (Keene et al., 1986)
 454 and EFs were close to 1, showing that Cl^- is almost 100% marine assuming that most of the sodium is from
 455 a marine source (Cao et al., 2009). Na^+ and Cl^- generally originate from sea-salt associated with oceanic
 456 air masses (Niu et al., 2013). Na^+ and Cl^- are highly correlated ($r=0.94$, $r=0.82$, $r=0.83$) (Figure 3) in Abidjan,
 457 Lamto and Korhogo respectively and suggest that both ions are mainly of marine origin. The $\text{Mg}^{2+}/\text{Na}^+$
 458 ratios calculated in Abidjan and Korhogo are close to the seawater reference value and also the EF values
 459 are equal to 1.

460 This result suggests a marine origin of Mg^{2+} at Abidjan and Korhogo. This result is supported by the strong
 461 correlations calculated between Mg^{2+} and Na^+ , and Mg^{2+} and Cl^- respectively ($r=0.82$) and ($r=0.94$) for
 462 Abidjan, and ($r=0.64$) and ($r=0.62$) for Korhogo (Figure 3).

463

464

465



466
 467
 468 Figure 3: Spearman matrix correlation of rainwater VWM concentrations ($\mu\text{eq. L}^{-1}$) for Abidjan, Lamto and Korhogo.
 469
 470



471 SSF and NSSF calculations indicate that for Abidjan and Korhogo, 81% and 75% of Mg^{2+} is from a marine
472 origin and that 19% and 25% are from non-marine sources. Lamto presents also a Mg^{2+}/Na^+ ratio above the
473 seawater reference with an EF value close to 2 indicating an additional non-marine contribution. SSF and
474 NSSF Mg^{2+} fractions are estimated to be 35 % and 65 % respectively. In addition, we found that Mg^{2+} and
475 Ca^{2+} are highly correlated ($r=0.92$) (Figure 3) indicating a possible terrigenous origin. The SO_4^{2-}/Na^+ ,
476 K^+/Na^+ , Ca^{2+}/Na^+ ratios in rainwater at all the sites were found to be higher than the seawater ratios and
477 corresponding EF values were well above 1.

478 These high ratios and EF values indicate potential contributions from anthropogenic and crustal sources in
479 addition to the marine source (Conradie et al., 2016). SSF and NSSF calculations show that SO_4^{2-} at Abidjan,
480 Lamto and Korhogo is mostly non-marine in origin, with non-marine contributions of 85%, 90% and 84%,
481 respectively. The marine fraction for Cl^- , SO_4^{2-} , K^+ , Ca^{2+} , Mg^{2+} were estimated to be approximately 94%,
482 15%, 13%, 3 % and 81%, respectively at Abidjan, 92%, 10%, 5%, 2 % and 35%, respectively at Lamto, and
483 100%, 16%, 3%, 2% and 75% respectively at Korhogo. The marine contribution to the total ionic content
484 for the three sites was computed using the following equation:

$$485 \quad \text{Marine} = [Na^+] + SSF[Cl^-] + SSF[Mg^{2+}] + SSF[Ca^{2+}] + SSF[K^+] + SSF[SO_4^{2-}],$$

486 where SSF is sea salt fraction

487

488 and was estimated to be $65.69 \mu\text{eq. L}^{-1}$, $11.59 \mu\text{eq. L}^{-1}$, $25.46 \mu\text{eq. L}^{-1}$ representing a contribution of 34 %
489 in Abidjan, 14% in Lamto and 24% in Korhogo (Figure 4). The strong marine contribution in Abidjan is
490 likely to be related to the coastal location of the city, resulting in a strong influence of monsoon air masses
491 loaded in sea salt. Similar conclusions are described in several studies (e.g. Hoinaski et al., 2014; Xing et
492 al., 2017) where high concentrations of Na^+ , Cl^- and Mg^{2+} have been attributed to ocean proximity. We
493 found that the rural site of Lamto records the lowest marine contribution. To explain these results, air mass
494 origins influencing Abidjan, Lamto and Korhogo have been studied using back trajectory calculations from
495 the NOAA HYSPLIT model over the study period 2017-2020 at 1500 m of altitude (Figure 5).

496

497

498

499

500

501

502

503

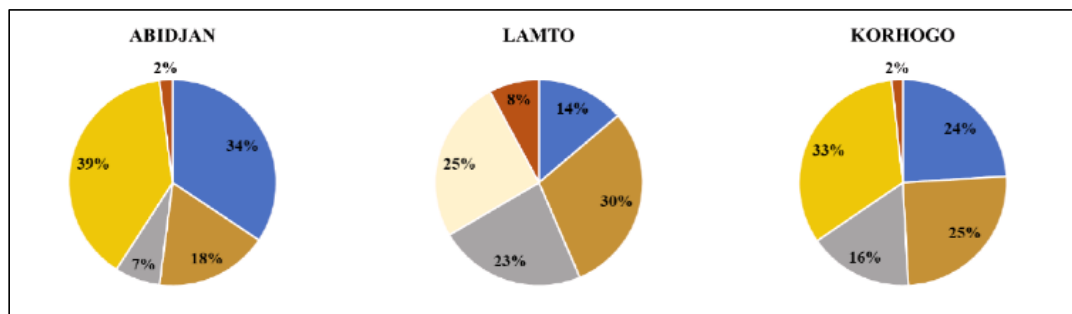
504

505

506

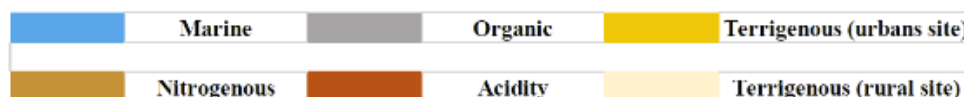


507



508

509



510

511

Figure 4: Estimation of marine, nitrogenous, organic, acidity and terrigenous contributions to rain chemical content along the Abidjan-Lamto-Korhogo transect (*terrigenous in this study represents a mixture of terrigenous and anthropogenic sources in urban areas, whereas in the rural Lamto site it represents a mixture of terrigenous and biomass burning sources)

516

517

518

519

520

521

522

523

524

525

526

527

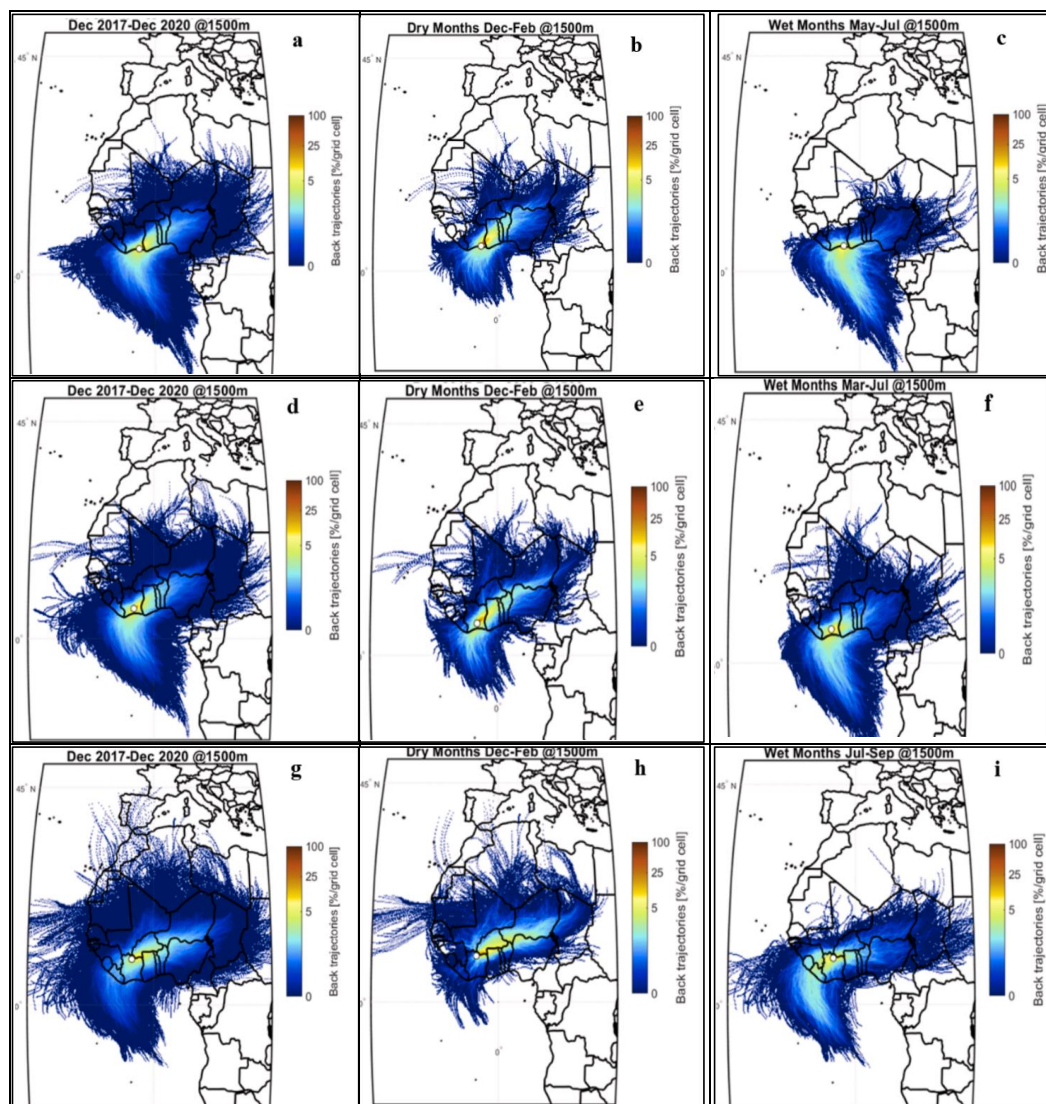
528

529

530

531

532



533

534 Figure 5: Overlay back-trajectory analyses for air masses arriving at the three sites for the study period (2017-2020).
535 a, d, g: average back-trajectory for the study period for Abidjan, Lamto and Korhogo, respectively. b, e, h: average
536 dry seasons back trajectory for the study period at Abidjan, Lamto and Korhogo respectively. c, f, i: average wet
537 seasons back-trajectory for the study period at Abidjan, Lamto and Korhogo respectively.
538

539 Results clearly indicate that the monsoonal oceanic air masses coming from the Guinean Gulf rich in sea-
540 salt aerosols influence the sites of Abidjan, Lamto and Korhogo (Figure 5-c, 5-f, 5-i). This influence is more
541 intense in Abidjan, indicated by a higher percentage of oceanic back trajectories indicated by light blue and
542 yellow cells (Figure 5-c) compared to Lamto with a lower percentage, indicated by a majority dark blue
543 cells (Figure 5-f). Despite its northernmost position and its greater distance from the coast, we found that



544 Korhogo is more influenced than Lamto by the marine source. Air mass back trajectories show that Korhogo
 545 is influenced both by oceanic air masses coming from the south and from the north-west border, this double
 546 contribution could explain the importance of the marine source contribution in Korhogo rainfall chemical
 547 content (figure 5-i). In West and Central Africa, convective rainfalls generally show a marine signature
 548 related to the boundary layer chemical content and a terrigenous signature from atmospheric levels above
 549 the boundary layer affected by continental air masses. Hot and dry continental air masses originating from
 550 the high-pressure system above the Sahara Desert give rise to dusty Harmattan winds over most of West
 551 Africa from November to February. In summer, moist equatorial air masses originating from the Atlantic
 552 ocean bring annual monsoon rains (Nicholson, 2013). Our results clearly identify these two chemical
 553 signatures during the monsoon season along the studied south-north transect represented by the Abidjan,
 554 Lamto, and Korhogo sites.

555

556 3.1.2. Terrigenous contribution

557 SO_4^{2-} , Mg^{2+} , K^+ and Cl^- ratios and crustal enrichments factors (EF) in relation to Ca^{2+} as an element of
 558 reference for crustal materials are presented in Table 3.

559

Sites	crustal water ratios (Keene et al 1986)	$\text{Cl}^-/\text{Ca}^{2+}$	$\text{SO}_4^{2-}/\text{Ca}^{2+}$	$\text{K}^+/\text{Ca}^{2+}$	$\text{Mg}^{2+}/\text{Ca}^{2+}$
		0.0031	0.0188	0.504	0.561
ABIDJAN	Ratios in rain	0.84	0.65	0.12	0.19
	$\text{EF}_{\text{CRUSTAL}}$	270	27	0.23	0.3
	NSSF (%)	6	85	87	19
LAMTO	Ratios in rain	0.58	0.48	0.20	0.26
	$\text{EF}_{\text{CRUSTAL}}$	26	26	0.1	0.5
	NSSF (%)	8	90	96	65
KORHOGO	Ratios in rain	0.44	0.93	0.28	0.61
	$\text{EF}_{\text{CRUSTAL}}$	141	49	0.26	1.1
	NSSF (%)	0	74	97	25

560

561

562

Table 3: Crustal Enrichment Factors in rains of Abidjan, Lamto and Korhogo.

563 $\text{SO}_4^{2-}/\text{Ca}^{2+}$ ratio values for the three sites are higher than the reference ratio and their EF values are well
 564 above 1. This result confirms that SO_4^{2-} in rain could be explained by marine, crustal and some potential
 565 additional sources. Marine contributions (SSF) of SO_4^{2-} have been estimated in the range of 10 to 16%
 566 along the transect Abidjan-Lamto-Korhogo and non-marine (NSSF) SO_4^{2-} contributions are estimated to be
 567 85 %, 90 %, 74 % for Abidjan, Lamto and Korhogo respectively. We hypothesize that urban site rainfall at
 568 Abidjan and Korhogo could be influenced by SO_4^{2-} of anthropogenic origin. SO_4^{2-} and NO_3^- often result



569 from anthropogenic emissions in urban areas (Keresztesi et al., 2020). SO_4^{2-} and NO_3^- concentrations in the
570 rainfall at the two urban sites are higher than those of Lamto (Table A1). In addition, we note that Abidjan
571 presents higher SO_4^{2-} concentrations ($19.50 \mu\text{eq. L}^{-1}$) compared to the other two sites. In using the ratio
572 $\text{SO}_4^{2-}/\text{NO}_3^-$, we are able to distinguish between mobile sources such as traffic sources and stationary sources
573 such as industry (Xu et al., 2015; Keresztesi et al., 2019). The $\text{SO}_4^{2-}/\text{NO}_3^-$ ratio at Abidjan is 1.87, which,
574 given the urban context, suggests the leading role of stationary sources e.g., industry or charcoal-burning
575 emissions from domestic combustion (Li et al., 2020; Naimabadi et al., 2018). However, the fuel for vehicles
576 used in West Africa and particularly in Côte d'Ivoire, contains high levels of sulfur (Marc et al., 2016).
577 Thus, high VWM SO_4^{2-} concentrations could be linked to traffic of motorized vehicles. In addition (Bahino
578 et al., 2018) have shown that SO_2 has three possible sources in Abidjan, i.e. traffic, domestic fire and waste
579 burning with traffic contributing the most.

580 Korhogo has a $\text{SO}_4^{2-}/\text{NO}_3^-$ ratio equal to 0.58 less than 1 illustrating the relative importance of NO_3^-
581 emissions compared to SO_4^{2-} . This result corroborates other rain chemical characteristics established at
582 Korhogo, which is considered a moderately industrialized city. In Abidjan, the importance of anthropogenic
583 emissions compared to the two other sites is explained by the level of population density, urbanization and
584 industrialization. Nevertheless, the SO_4^{2-} concentration in Abidjan precipitation is lower by a factor 2 or 3
585 than those recorded in megacities such as Hong Kong, Jiaozhou bay (China) and New Delhi (India) (Wai et
586 al., 2005; Tiwari et al., 2007; Xing et al., 2017) (Table 4).

587

588

589

590

591

592

593

594

595

596

597

598



599

Sites	period	n	pH	H ⁺	Ca ²⁺	Mg ²⁺	Na ⁺	K ⁺	NH ₄ ⁺	HCO ₃ ⁻	Cl ⁻	SO ₄ ²⁻	NO ₃ ⁻
Limeira, Brazil ^(a)	09/2013 – 03/2014	30	5.62	2.40	54.88	17.40	22.39	5.68	34.36	20.13	7.06	15.54	14.73
Jiaozhou Bay, China ^(b)	06/2015 – 05/2016	49	4.77	16.90	64.10	21.90	54.7	17.20	107.00	–	66.00	93.70	62.90
Juiz de Fora, Brazil ^(c)	2014	53	6.60	0.40	31.90	13.80	29.10	16.00	–	8.50	18.30	3.00	25.60
Lijiang City, China ^(d)	06/2012 – 11/2012	176	6.07	0.85	50.10	10.90	0.98	2.01	20.80	–	2.04	23.70	7.00
Djougou, Benin ^(e)	2006–2009	530	5.10	6.46	13.30	2.10	3.80	2.00	14.30	–	3.40	6.20	8.20
Florianópolis, Brazil ^(f)	08/2006 – 11/2006	22	4.97	10.71	7.98	9.00	59.80	3.14	–	–	56.94	9.94	15.18
Ibiúna, Brazil ^(g)	2006	15	6.23	0.59	114.00	10.10	37.70	8.25	56.70	–	21.20	60.90	21.80
Delhi, Índia ^(h)	2003–2005	355	6.39	1.02	80.88	23.11	24.35	14.18	31.81	38.42	29.52	40.81	25.17
Porto Alegre, Brazil ⁽ⁱ⁾	2005–2007	177	5.30	4.98	22.40	9.28	18.40	6.48	35.30	–	16.10	22.10	3.95
Guaíba, Brazil ^(j)	01/2002 – 12/2002	70	5.72	1.90	8.41	3.85	11.10	2.81	28.10	–	6.98	13.20	2.47
Ilha Grande, Brazil ^(k)	03/2002 – 09/2002	20	5.22	6.00	9.20	40.40	142.20	7.10	9.90	–	178.20	34.80	12.00
São Paulo, Brazil ^(l)	01/2003 – 12/2003	44	5.39	4.03	21.60	6.60	8.64	9.55	37.10	–	9.29	23.80	20.10
Ankara, Turkey ^(m)	09/1994 – 12/1996	162	6.33	1.60	71.4	9.30	15.60	9.8	86.40	–	20.40	48.00	29.20
Southern Taiwan ⁽ⁿ⁾	05/2005 – 12/2008	402	***	–	53.40	32.60	97.10	10.90	50.20	119.60	63.10	40.50	15.70
Newark, USA ^(o)	2006 – 2007	46	4.60	25.0	6.00	3.30	10.90	1.30	24.40	–	10.70	38.10	14.40
Hong Kong, China ^(p)	10/1998 – 10/2000	156	4.20	63.20	16.20	7.00	36.90	4.20	22.00	–	42.40	70	27.60
Abidjan, Côte d'Ivoire ^(q)	2019–2020	165	5.78	3.90	25.00	5.80	21.50	3.60	19.01	5.00	24.30	19.50	8.70
Lamto, Côte d'Ivoire ^(r)	2019–2020	146	5.31	6.57	9.91	2.57	5.41	2.00	17.90	1.50	5.57	4.76	7.22
Korogho, Côte d'Ivoire ^(s)	2019–2020	97	5.57	4.09	20.09	3.40	11.24	8.63	17.38	2.30	9.57	5.27	9.90

600

601 Table 4: Average VWM ($\mu\text{eq. L}^{-1}$) in rainwater in Abidjan, Lamto and Korhogo, Côte d' Ivoire (this study) and other
 602 places in the world (adapted from (Martins et al., 2018))

603

604 The $\text{K}^+/\text{Ca}^{2+}$ ratios are below the reference crustal value and the EF values are above 1 for all three sites. In
 605 addition, K^+ and Ca^{2+} are highly correlated with r value of ($r=0.79$), ($r=0.70$), ($r=0.73$) (Figure 3)
 606 respectively at Abidjan, Lamto and Korhogo. These results indicate a possible terrigenous origin of K^+ . The
 607 NSSF K^+ fraction was found to be 87%, 96% and 97 % at Abidjan, Lamto and Korhogo respectively (Table
 608 4). However, a strong correlation coefficient between Cl^- and K^+ with ($r=0.75$), ($r=0.71$) and $r= (0.86)$ found
 609 respectively at Abidjan, Lamto and Korhogo could suggest a potential K^+ origin from biomass combustion,
 610 which is a source of KCl (Lara et al., 2001). Since Submicron K^+ is considered to be an atmospheric tracer
 611 of biomass combustion (Andreae et al., 1998; de Mello, 2001), in the urban context of Abidjan and Korhogo
 612 we can attribute household fire burning using charcoal as source of K^+ whereas in Lamto biomass burning
 613 of vegetation is likely to be the main source of K^+ .

614



615 Calculations of Mg^{2+} marine, non-marine and crustal ratios (SSF and NSSF) and EFs indicate that the
616 terrigenous contribution of this ion is limited to 19% at Abidjan and 25% at Korhogo while it represents
617 65% at Lamto with a strong correlation between Ca^{2+} and Mg^{2+} ($r=0.92$). NSSF of Ca^{2+} are 97 %, 98% and
618 98% respectively at Abidjan, Lamto and Korhogo. Ca^{2+} displays high correlations with SO_4^{2-} ($r=0.86$),
619 ($r=0.76$), ($r=0.91$), Mg^{2+} ($r=0.81$), ($r=0.92$), ($r=0.91$) and K^+ ($r=0.79$), ($r=0.70$), ($r=0.73$) respectively at
620 Abidjan, Lamto and Korhogo. We found that Ca^{2+} is the most important ion in the rainwater composition
621 measured at Abidjan and Korhogo with a concentration of $38.30 \mu eq. L^{-1}$, $20.09 \mu eq. L^{-1}$ respectively. At
622 Lamto it is the third most important ion with a concentration of $9.91 \mu eq. L^{-1}$. The Ca^{2+} predominance in
623 rain at the urban sites (Abidjan and Korhogo) could be explained by a contribution of multiple sources. In
624 Abidjan, the expansion of construction activities involving cement production represents a potential source
625 of Ca^{2+} particles (Shakya et al., 2017; Samara et al., 2000; Khwaja et al., 1990). In addition, soil particle
626 resuspension from road dust can also contribute to the precipitation Ca^{2+} content in precipitation (Tiwari, et
627 al., 2007 ; Fernandes et al., 2012 ; Kulshrestha et al., 2003 ; Riccio et al., 2017). To further investigate the
628 pattern of VWM Ca^{2+} concentration in rainwater, we analyzed Hysplit air mass back-trajectories at specific
629 dates (Abidjan: 10 April 2020, Lamto: 6 march 2020, Korhogo: 28 march 2019) representative of a
630 maximum Ca^{2+} VWM concentrations of $555 \mu eq. L^{-1}$, $231 \mu eq. L^{-1}$ and $164 \mu eq. L^{-1}$ for Abidjan, Lamto and
631 Korhogo respectively (Figure 6). At the transition between the dry and the wet season (march-April), we
632 observe that north east air masses coming from the Saharan desert at 2500 m of altitude are heavily loaded
633 with dust particles rich in terrigenous chemical components (such as Ca^{2+}) which affects all the three sites.
634 The scavenging of these particles by rainy events at the seasonal transition explains the magnitude of VWM
635 Ca^{2+} concentrations recorded in rainwater at the three sites at the beginning of the wet season. with
636 concentrations ranged from 3.95 to $555 \mu eq. L^{-1}$, 1.2 to $231 \mu eq. L^{-1}$ and 1 to $164 \mu eq. L^{-1}$ at Abidjan, Lamto
637 and Korhogo respectively.

638

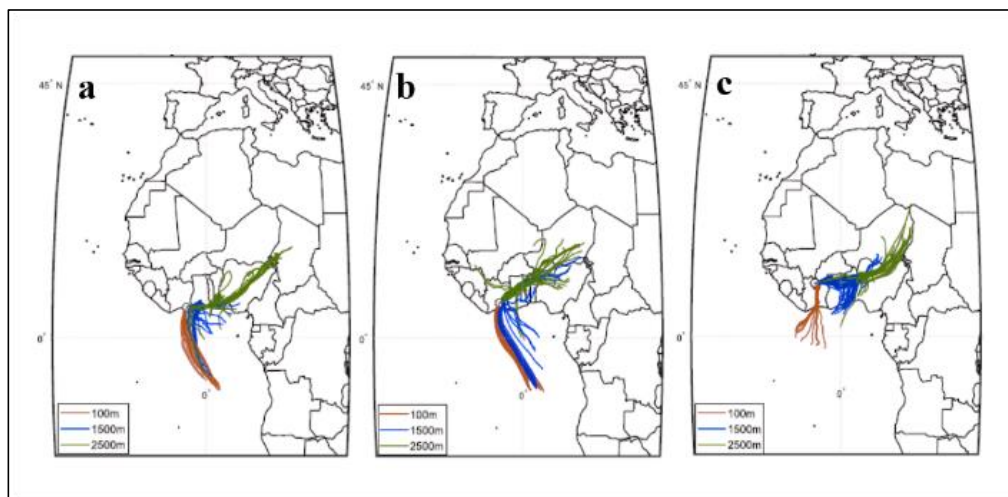
639

640

641

642

643



644
645
646
647
648

Figure 6: 96-hour overlay back-trajectories initiated in Abidjan (a: Abidjan: 10 April 2020), Lamto (b: 6 March 2020) and Korhogo (c: 28 March 2019)

649 The terrigenous signature identified at African sites emphasizes the direct influence of soil dust on rainfall
650 (Laouali et al., 2021). The North African desert areas (Sahel and Sahara) are probably the most important
651 mineral aerosol source (Kaufman, 2005; Marticorena et al., 2010) and when the monsoon sets in, North East
652 Harmattan air masses heavily loaded in soil dust terrigenous components are transported over the continent.
653 Due to the partial dissolution of soil dust, rain is loaded with dissolved calcium and carbonates (calcite),
654 dolomite, gypsum and also illite, smectite or palygorskite which explains the enrichment of Ca^{2+} , SO_4^{2-} ,
655 Mg^{2+} and K^+ (Avila et al., 1997).

656 This result is similar to those obtained in other African ecosystems (Galy-Lacaux and Modi, 1998; Sigha-
657 Nkamdjou et al., 2003; Galy-Lacaux et al., 2009; Laouali et al., 2012; Akpo et al., 2015) and other regions
658 of the world including Asia (Tiwari et al., 2016). At Korhogo, the traffic and industrial sources of
659 terrigenous Ca^{2+} are certainly lower compared to Abidjan. We presume that the Ca^{2+} terrigenous
660 contribution is primarily related to Saharan dust transport that is predominant at Korhogo located in the
661 northern climatic zone influenced by warm and dry air masses (Harmattan) during the boreal winter
662 (Marticorena et al., 2010) (Figure 5-h). Lamto rains present the lowest Ca^{2+} VWM concentration ($9.91 \mu\text{eq. L}^{-1}$)
663 over the studied transect and the lowest terrigenous contribution. This result is comparable with that of
664 Yoboué et al., (2005) ($9.20 \mu\text{eq. L}^{-1}$) and may be explained by the position of Lamto, which is located in the
665 climatic center zone and appeared to be less influenced by the Harmattan air masses than Korhogo as shown
666 by air mass back trajectories analysis (Figure 5-d,5-g).

667
668



669 Ca^{2+} has a significant impact on the acidity neutralizing potential of precipitation and consequently it would
670 be useful to compare the concentration established in Côte d'Ivoire with concentrations in the rest of the
671 world (Table 4). Abidjan, Lamto and Korhogo record a Ca^{2+} VWM concentration lower than cities such as
672 New Delhi (India) ($80.88 \mu\text{eq. L}^{-1}$), Limeira (Brazil) ($54.88 \mu\text{eq. L}^{-1}$) and Ankara (Turkey) ($71.40 \mu\text{eq. L}^{-1}$),
673 that present a VWM concentrations ranging from 55 to $80 \mu\text{eq. L}^{-1}$ of Ca^{2+} . However, Ca^{2+} concentrations
674 in Côte d'Ivoire are higher than those of Florianopolis, Brazil ($7.98 \mu\text{eq. L}^{-1}$) and Newark (USA) ($6.00 \mu\text{eq. L}^{-1}$).
675 Thus, highly urbanized and industrialized cities with a dense demography, like the megacity of Abidjan,
676 will tend to have higher Ca^{2+} and SO_4^{2-} concentrations as a result of industrial activities, vehicle emissions
677 (including road resuspension) and other emissions related to urban activities (Hoinaski et al., 2013). The
678 medium-sized city of Korhogo, less urbanized and industrialized than Abidjan and the rural, wet-savanna
679 site of Lamto are more influenced by continental air mass transport from African deserts.

680 The contribution of terrigenous compounds is computed according to the equation: $\text{NSS}[\text{Ca}^{2+}] + \text{NSS}[\text{Mg}^{2+}]$
681 $\text{NSS}[\text{K}^+] + \text{NSS}[\text{SO}_4^{2-}] + \text{Tcarb}$. It is estimated to be $74.21 \mu\text{eq. L}^{-1}$, $21.61 \mu\text{eq. L}^{-1}$, and $37.25 \mu\text{eq. L}^{-1}$ and
682 contribute to 39 %, 25%, 33% of the total ionic content respectively for Abidjan, Lamto and Korhogo. We
683 must specify that the so-called terrigenous contribution in this study represents a mixture of terrigenous and
684 anthropogenic sources in urban areas, whereas at the rural site of Lamto, it represents a mixture of
685 terrigenous and biomass burning sources (Figure 4). Abidjan and Korhogo present higher deposition fluxes
686 of terrigenous ionic compounds such as calcium with annual averages of $11.32 \pm 6.27 \text{ kg ha}^{-1} \text{ yr}^{-1}$, and $4.50 \pm$
687 $2.07 \text{ kg ha}^{-1} \text{ yr}^{-1}$ respectively. Ca^{2+} deposition fluxes in Lamto are lower with an annual average value of
688 $2.59 \pm 0.31 \text{ kg ha}^{-1} \text{ yr}^{-1}$. This may reflect the difference between the urban site and rural site in term of acid
689 buffering capacities of rainwater with the urban sites of Abidjan and Korhogo more heavily affected by this
690 phenomenon than the rural site of Lamto.

691

692 3.1.3. Nitrogenous contribution

693 Nitrogenous contribution, defined as the sum of ammonium and nitrate VWM concentrations $[\text{NH}_4^+] +$
694 $[\text{NO}_3^-]$, is respectively estimated to be $33.70 \mu\text{eq. L}^{-1}$, $25.12 \mu\text{eq. L}^{-1}$, and $26.47 \mu\text{eq. L}^{-1}$, representing 18
695 %, 30 % and 25% of the total precipitation composition at Abidjan, Lamto and Korhogo respectively.
696 Abidjan's rainfall composition exhibits the weakest nitrogenous contribution. However, Abidjan records
697 the highest VWM concentrations of nitrogenous species with NH_4^+ VWM concentration value of $22.60 \mu\text{eq. L}^{-1}$
698 or 67% and NO_3^- VWM concentration value of $11.10 \mu\text{eq. L}^{-1}$ or 32 %.

699 In the context of urbanization and demographic growth, the development of fossil-fuel combustion from
700 road traffic and domestic combustion may play an important role in NH_3 and NO_2 emissions (Ehrnsperger
701 and Klemm, 2021). Similarly, (Bahino et al., 2018) state that NO_2 gas emissions in Abidjan have two



702 distinct sources: (i) the limited traffic of garbage collection vehicles, and the circulation of mini buses called
703 “Gbaka”, which connect the city center to the suburbs, with average concentration levels of 17.8 ± 4.7 ppb,
704 and (ii) industrial activities, with average concentration levels of 20.9 ± 2.8 ppb. In contrast, NH_3 gas
705 emissions are strongly linked to biomass burning (firewood and charcoal) as a source of energy by most
706 households, with average concentration levels of 84.9 ± 17.9 ppb, and emissions from waste burning, with
707 average concentration levels of 39 ppb in Abidjan.

708 Lamto exhibits the highest nitrogenous contribution, representing one third of its rainfall composition,
709 consisting of 71% NH_4^+ and 29 % NO_3^- . The high NH_4^+ concentration could be explained by the rural
710 features of Lamto, such as bacterial decomposition of urea in animal excreta and emissions from natural or
711 fertilized soils by agriculture activities, which are both sources of NH_3 (Schlesinger and Hartley, 1992; Galy-
712 Lacaux and Modi, 1998). As noted by Suzanne et al., (2016), agricultural activity contributes to substantial
713 NH_3 gas emissions, resulting from the use of large quantities of fertilizers and plant phytosanitary product
714 to increase rubber and cocoa harvests around Lamto. Savanna fires and household fuelwood burning are
715 also primary sources of NH_3 (Delmas et al., 1995). Strong correlations of both NH_4^+ and NO_3^- with SO_4^{2-}
716 ($r=0.72$ and $r=0.77$ respectively) (Figure 3) indicate that NH_4^+ is related to multiphase reactions in the
717 atmosphere. Most of the time ammonia exists in multiple form of aerosols in the atmosphere as $(\text{NH}_4)_2\text{SO}_4$,
718 NH_4HSO_4 , NH_4NO_3 and NH_4F (Seinfeld, 1986; Zhang et al., 2007a). The relatively low NO_3^- VWM
719 concentration measured at Lamto could be explained by the low biogenic NO_x emissions in the Lamto
720 station according to (Serça et al., 1998). Further, (Akpo et al., 2015) propose that NO_3^- in rainwater could
721 be the result of gas-phase transformations of NO_x to HNO_3 , followed by a reaction with NH_3 to form
722 NH_4NO_3 .

723 Nitrogenous concentration values measured at Lamto in this study for the period 2019-2020 are in the same
724 range as those found in the study of Yoboué et al., (2005) from 1995-2002 , with $17.6 \mu\text{eq. L}^{-1}$ of NH_4^+ and
725 $7.7 \mu\text{eq. L}^{-1}$ of NO_3^- . The nitrogenous contribution at the Korhogo site represents the second most important
726 contribution to the rain chemical content. NH_4^+ is dominant (71%) compared to NO_3^- (29%). This result is
727 likely related to combined rural and urban characteristics of Korhogo, which allow a mixture of sources.
728 NH_4^+ concentrations are likely related to both the emissions of NH_3 from household charcoal burning
729 (Dentener and Crutzen ,1994; Zhang et al., 2007) , as well as biomass burning and the use of N-fertilizer in
730 agriculture around Korhogo (Galy-Lacaux and Modi, 1998; Laouali et al., 2012; Delmas et al., 1995). The
731 ratio $\text{SO}_4^{2-}/\text{NO}_3^-$ has a value of 0.53, which may indicate a substantial mobile source contribution (Rao et
732 al., 2017).It is worth recalling that two-wheeled vehicles are predominant in Korhogo and could be a
733 possible source of NO_2 gases (Roger et al., 2016).VWM concentrations of nitrogenous species (NH_4^+ , NO_3^-
734) measured in this study are smaller than the values of cities such as Sao Paulo, Brazil ($37.10, 20.00 \mu\text{eq. L}^{-1}$)
735 1); New Delhi, India ($31.81, 25.17 \mu\text{eq. L}^{-1}$); and Jiaozhou Bay, China ($107, 62.90 \mu\text{eq. L}^{-1}$), and are slightly
736 higher than the value of the West African rural site of Djougou in Benin ($14.30, 8.20 \mu\text{eq. L}^{-1}$) (Table 4).



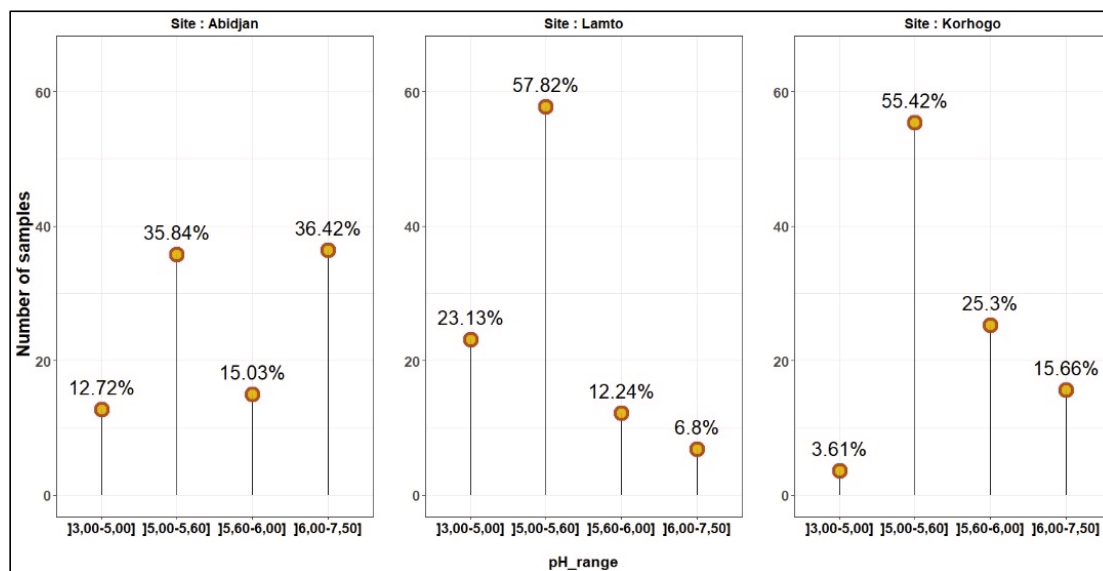
737 Thus, the level of NH_4^+ VWM concentration in Côte d'Ivoire and in Benin are largely lower than the levels
738 recorded in urban areas such as in Brazil or in China where urbanization, fossil fuel consumption and
739 industrialization of agriculture (including intensive use of fertilizers and animals' manures) surroundings
740 cities are more significant (Migliavacca et al., 2005).

741 In the two rural wet savanna sites of Lamto and Benin, VWM NH_4^+ concentrations are attributed mainly to
742 livestock breeding, biomass burning, and, to some extent, agricultural activities (Zhang et al., 2007).
743 Nitrogen is considered to be an important source of nutrients in ecosystems, however, levels above a certain
744 critical load, which depends on the specific ecosystem, can be considered to be contributing to pollution and
745 eutrophication of the environment (Bobbink et al., 2010; Josipovic et al., 2011). We have calculated the
746 total annual nitrogen wet deposition fluxes for the three sites, finding values of $7.01 \text{ kg N ha}^{-1} \text{ yr}^{-1}$, 4.61 kg
747 $\text{N ha}^{-1} \text{ yr}^{-1}$, and $4.18 \text{ kg N ha}^{-1} \text{ yr}^{-1}$ respectively for Abidjan, Lamto and Korhogo. We may conclude that
748 nitrogen wet deposition fluxes in the megacity of Abidjan are relatively more important than in the rural
749 area of Lamto and the regional/local connector city of Korhogo. In addition, we emphasize that annual
750 nitrogen wet deposition fluxes at the three sites are dominated by N-NH_4^+ with wet deposition fluxes of 4.68
751 $\text{kg N ha}^{-1} \text{ yr}^{-1}$, $3.27 \text{ kg N ha}^{-1} \text{ yr}^{-1}$, and $2.73 \text{ kg N ha}^{-1} \text{ yr}^{-1}$ respectively. N-NO_3^- deposition flux values are
752 lower by a factor of two, with values of $2.33 \text{ kg N ha}^{-1} \text{ yr}^{-1}$, $1.34 \text{ kg N ha}^{-1} \text{ yr}^{-1}$, and $1.45 \text{ kg N ha}^{-1} \text{ yr}^{-1}$
753 respectively at Abidjan, Lamto and Korhogo. The values of nitrogen wet deposition remain lower than the
754 critical load, estimated to be $10 \text{ kg N ha}^{-1} \text{ yr}^{-1}$, which is defined as the highest load that will not cause
755 chemical changes leading to long-term harmful effects on the most sensitive ecological systems (Nilsson,
756 1988; Bobbink et al., 2010). We can conclude that the three sites are not exposed to potential risks of
757 eutrophication or acidification of their environment for the moment. However, further investigations need
758 to be undertaken to assess total nitrogen deposition, including both wet and dry processes as well as the
759 evolution of those fluxes in the future.

760

761 3.1.4. pH and Acid contribution

762 Mean pH measurements for the three studied sites over the period 2018-2020 are given in Table A1 while
763 Figure 7 presents the pH frequency distribution.



764

765 Figure 7: Frequency distribution of pH values of Abidjan, Lamto and Korhogo rainwater for the study period.
766

767 The mean pH is 5.76 ± 0.59 , 5.31 ± 0.32 and 5.57 ± 0.30 respectively at Abidjan, Lamto and Korhogo. Mean
768 VWM H^+ concentrations, calculated from annual mean precipitation pH are estimated to be $4.1 \pm 0.10 \mu\text{eq.}$
769 L^{-1} , $6.57 \pm 0.04 \mu\text{eq. } L^{-1}$ and $4.09 \pm 1.7 \mu\text{eq. } L^{-1}$ at Abidjan, Lamto and Korhogo respectively (Table A1).
770 The reference pH of rainwater is 5.6 representing the acidity of the pure water in equilibrium with the
771 atmospheric CO_2 concentration (Charlson and Rodhe, 1982; Galloway et al., 1982). Acid rain is defined as
772 rain with pH below the threshold of 5.60 (Drever et al., 1997). Results show that for the study period of
773 2018-2020, 51 % of the 173 rain events whose pH values were measured in Abidjan, present an acidic pH
774 lower than 5.6, while 49% have an alkaline pH (>5.6). At Lamto, precipitation is mainly acidic with 81%
775 of the 148 rainfall samples having a pH value measured below 5.6.

776 At Korhogo, precipitation was slightly acidic with 59% of the 83 rainfall samples having measured pH
777 values below 5.6. This result is similar to the study of (Payus et al.2020) where rural areas recorded higher
778 acidity of precipitation, with a total average pH of 5.54 ± 0.39 compared to urban areas with a total average
779 pH of 5.77 ± 0.26 . Abidjan precipitation presented a pH value close to cities such as Guiaba, Brazil (5.72),
780 Lijiang city, China (6.07) and Ibuina, Brazil (6.23) and Korhogo has a pH value similar to cities such as
781 Limeira (5.62) (Table 5). In comparison to others rural ecosystems, Lamto has a pH value close to Djougou
782 (5.10) but lower than those of Sahelian sites such Katibougou (5.54), Dahra (6.10) and Agoufou
783 (6.28)(Laouali et al., 2021).

784 Electrical conductivity (EC) of rainwater relies on total soluble components and lower EC values reflect
785 better atmospheric environmental quality (Zhang et al., 2007). Mean EC values of precipitation measured



786 at Abidjan, Lamto and Korhogo ranged from 0 to 169 $\mu\text{S cm}^{-1}$, with means of 21.36 $\mu\text{S cm}^{-1}$, 6 $\mu\text{S cm}^{-1}$ and
787 5.9 $\mu\text{S cm}^{-1}$ respectively. Based on this observation, EC rain characteristics emphasize lower environmental
788 quality of Abidjan, a polluted megacity compared to Korhogo and Lamto.

789 The contribution of mineral acidity, mainly related to the incorporation of H_2SO_4 and HNO_3 is 69%, 38%
790 and 52% respectively at Abidjan, Lamto and Korhogo while organic acids represent 31 %, 62% and 48 %
791 of acidity respectively at each site (Table 5). Abidjan and Korhogo are mainly influenced by mineral acidity
792 whereas Lamto show a high organic contribution (Table 5). The patterns observed at the urban sites are
793 comparable to measurements made in other African ecosystems, especially in South African dry savannas
794 influenced by anthropogenic sources (Mphepya et al., 2004; Conradie et al., 2016).

795 In figure 4, the organic contribution is computed according to the equation: $[\text{SO}_4^{2-}] + [\text{NO}_3^-] + [\text{HCOO}^-] +$
796 $[\text{CH}_3\text{COO}^-] + [\text{C}_2\text{H}_5\text{COO}^-] + [\text{C}_2\text{O}_4^{2-}]$, with values representing 7 %, 23% and 16 % of the source's
797 contributions to the chemical content of rainfall in Abidjan, Lamto and Korhogo respectively. The relatively
798 low organic acidity in Abidjan is likely related to the fact that in urban areas, anthropogenic activities are
799 the main contributors of acid rain (Radojevic and Harrison, 1992; Park et al., 2015; Payus et al., 2020).
800 However, organic acids can be emitted in the urban environment, mainly from motorized vehicles. In the
801 study of (Dominutti et al., 2019) in Abidjan, the majority of VOCs (Volatile organic carbon) which are
802 precursors of organic acids (Guenther, et al. 2013) are attributed to domestic fires, landfill fires and traffic
803 sources. At Lamto, the high acidity contribution confirms results previously established by (Yoboué et al.
804 2005) (56% organic and 44% mineral contributions). However, our study shows that the organic
805 contribution has increased compared to the period 1995-2002 studied by Yoboué et al., (2005).

806 The annual VWM concentration of HCOO^- , CH_3COO^- and $\text{C}_2\text{O}_4^{2-}$ at Lamto are higher than at the urban
807 sites, especially for HCOO^- . The contribution of organic acidity in precipitation is mainly due to VOC
808 emissions from biomass burning and from the vegetation in rural sites (Guenther et al., 2006; Galy-Lacaux
809 et al., 2009; Vet et al., 2014). Despite acidity in Korhogo being dominated by the mineral acidity, there is
810 significant contribution from organic acidity. This configuration could be related to the singularity of the
811 urban site of Korhogo, which has a certain rural characteristic supporting a mixture of natural sources of
812 VOC, such as emissions from biomass burning and vegetation, and from anthropogenic sources such as
813 motorized vehicles. This result is similar to those found in the study of (Sun et al., 2016).

814 The neutralization Factor (NF) of mineral and organic acids by bases such as anions (oxides, carbonates or
815 bicarbonates, etc.) associated with base cations such as Ca^{2+} , NH_4^+ , Mg^{2+} , K^+ can be evaluated by using Eq
816 10 (Possanzini et al., 1988; Kulshrestha et al., 2003). Abidjan presents NF values for Ca^{2+} , NH_4^+ , K^+ , Mg^{2+}
817 of 0.87, 0.41, 0.10, and 0.21 respectively, revealing that Ca^{2+} is the most important ion in neutralizing
818 acidity, followed by NH_4^+ . At Korhogo and Lamto, both Ca^{2+} (NF=0.64 and 0.32) and NH_4^+ (NF=0.57 and
819 0.58) ions are also the major ions that neutralized acids in rains. In Lamto, the importance of NH_4^+ as the



820 main neutralizing factor is emphasized but the strong correlations between NH_4^+ and organic acids (HCOO^-
821 , CH_3COO^- , $\text{C}_2\text{O}_4^{2-}$) respectively equal to $r=0.92$, $r=0.90$, and $r=0.89$.

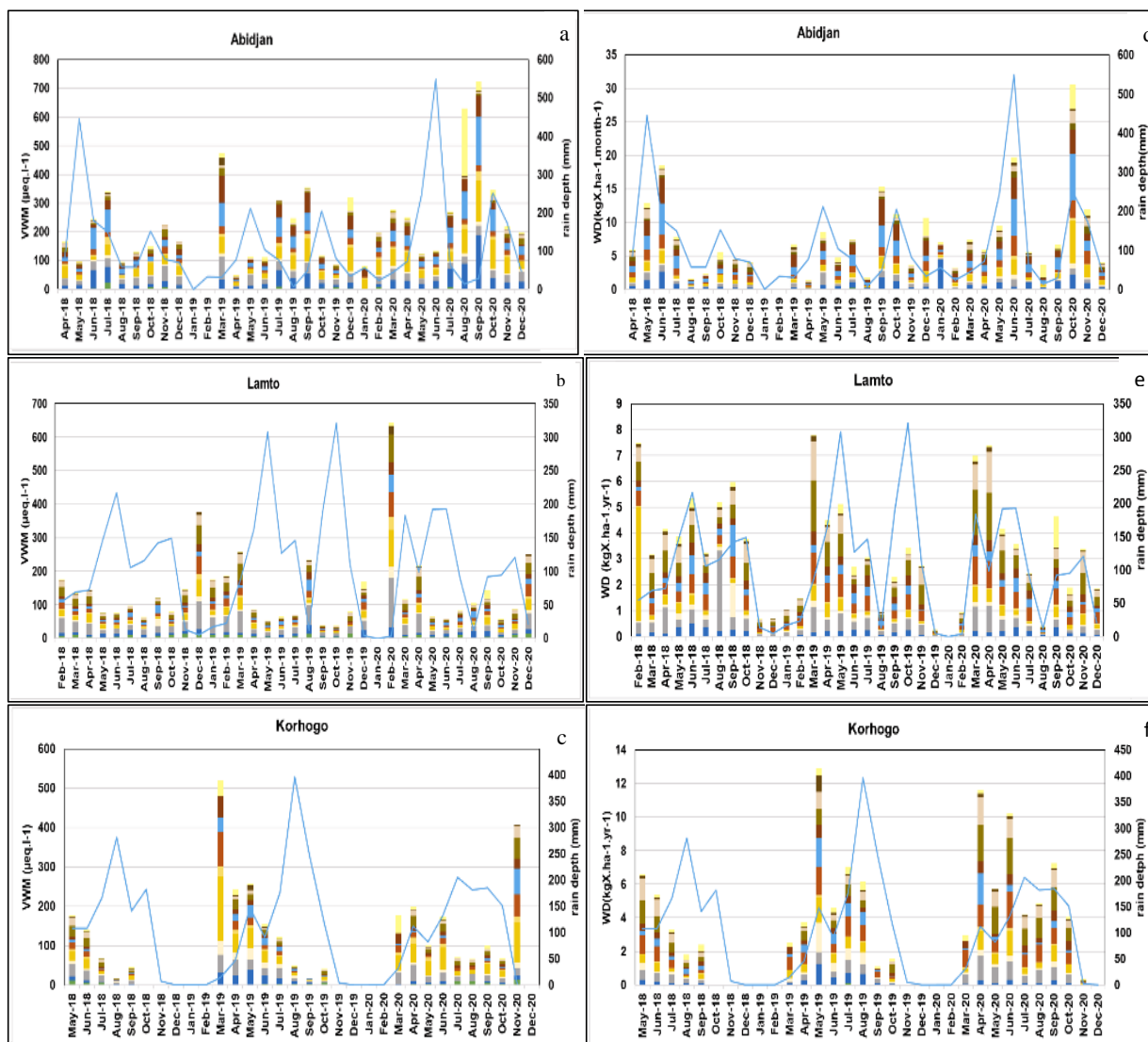
822 Considering the equations of section 2.5, we calculated the Fractional Acidity (FA) to evaluate the
823 neutralizing strength of acidifying compounds Eq 9 (Balasubramanian et al., 2001). The average FAs for
824 the studied period (2019-2020) at Abidjan, Lamto and Korhogo are estimated to 0.11, 0.21 and 0.13. It
825 indicates that 89%, 79% and 87% of the rain acidity has been neutralized by alkaline substances at Abidjan,
826 Lamto and Korhogo respectively. According to (Sigha-Nkamdjou et al. 2003) who defined Potential acidity
827 (pA) as the sum of potential acidic compounds in the form of mineral and organic acids, we calculate pAs
828 equal to $44.11 \mu\text{eq. L}^{-1}$ at Abidjan, $31.40 \mu\text{eq. L}^{-1}$ at Lamto and $36.0 \mu\text{eq. L}^{-1}$ at Korhogo. The measured
829 acidity ($4.10 \mu\text{eq. L}^{-1}$, $6.57 \mu\text{eq. L}^{-1}$ and $4.09 \mu\text{eq. L}^{-1}$) is lower by a factor of 3 to 10 compared to calculated
830 pA. In order to explain this gap, we assess the balance between neutralization and acidification processes in
831 rainwater chemistry by using Eq11. NP/AP values are respectively 1.36, 0.90, and 1.30 for Abidjan, Lamto
832 and Korhogo. Thus, we emphasize that neutralization processes are much more significant in the rainwater
833 chemistry of the urban sites of Abidjan and Korhogo compared to the rural site of Lamto ($\text{NP/AP} < 1$).
834 Consequently, neutralization processes explain the differences between the potential H^+ and the measured
835 acidity in precipitation collected over Côte d'Ivoire's sites.

836 3.2. Monthly and seasonal concentration variation of major ions in rainwater 837

838 The monthly VWM ionic concentrations and WD are presented in Figure 8 (a-f) and Fig.A2. Results exhibit
839 seasonality at all three sites. During the dry season the ionic load are higher compared to the wet season.
840 Indeed, the first rains of the year (February-March in Abidjan, February in Lamto, March in Korhogo) at
841 each site show very high ionic load. The same result is obtained for the inter-seasons months from June to
842 September at Abidjan and for the last months of rain (November December) at all three sites. This observed
843 relationship between rainfall and VWM ions concentrations in rainwater is related to the atmosphere having
844 high levels of gas and particle scavenging at the beginning of the rainy season, but the gases and particles
845 are not highly diluted because of the small amounts of rain (Huang et al., 2009).

846

847



848
849

	t carb
	C ₂ O ₄ ²⁻
	C ₂ H ₃ COO ⁻
	CH ₃ COO ⁻
	HCOO ⁻
	SO ₄ ²⁻
	Cl ⁻
	NO ₃ ⁻
	Mg ²⁺
	Ca ²⁺
	K ⁺
	NH ₄ ⁺
	Na ⁺
	H ⁺
	lit

850

851 Figure 8: Monthly VWM concentrations of major ions (µeq. L⁻¹) at Abidjan (a), Lamto (b) and Korhogo
 852 (c) and monthly wet deposition (WD) fluxes (kgX.ha⁻¹. yr⁻¹) at Abidjan (e), Lamto (f) and Korhogo (g)

853



854 Monthly VWM concentrations variations of main ionic in Abidjan is dominated in the decreasing order by
855 Ca^{2+} , Cl^- , Na^+ , NH_4^+ , SO_4^{2-} with values ranging respectively from 5.14 to 143.52 $\mu\text{eq. L}^{-1}$, from 4.01 to
856 166.47 $\mu\text{eq. L}^{-1}$, 3.72 to 185.79 $\mu\text{eq. L}^{-1}$, from 6.96 to 82.52 $\mu\text{eq. L}^{-1}$ and from 3.41 to 93.89 $\mu\text{eq. L}^{-1}$. Lamto
857 is dominated in the decreasing order by NH_4^+ , HCOO^- , Ca^{2+} , NO_3^- , Cl^- with values ranging respectively
858 from 6.14 to 146. $\mu\text{eq. L}^{-1}$, from 3.28 to 83.91 $\mu\text{eq. L}^{-1}$, from 2.42 to 108.14 $\mu\text{eq. L}^{-1}$, from 2.83 to 72.72
859 $\mu\text{eq. L}^{-1}$ and from 1.21 to 51.91 $\mu\text{eq. L}^{-1}$.

860 Korhogo presents in term of monthly VWM concentration the same dominants ions but with different order
861 of importance and so Korhogo is dominated in the decreasing order by Ca^{2+} , NH_4^+ , NO_3^- , HCOO^- and Cl^-
862 with values ranging respectively from 0.78 to 164.33 $\mu\text{eq. L}^{-1}$, from 3.61 to 44.74 $\mu\text{eq. L}^{-1}$, from 0.69 to
863 88.62 $\mu\text{eq. L}^{-1}$, from 0.25 to 52.53 $\mu\text{eq. L}^{-1}$ and from 1.09 to 65.98 $\mu\text{eq. L}^{-1}$. Conversely, Wet deposition (WD)
864 show an opposite trend compared to monthly VWM concentration distribution with maximum WD during
865 the wet seasons in all three sites (Figure 8). Monthly wet deposition fluxes at Abidjan are dominated by the
866 following ions in decreasing order Cl^- , SO_4^{2-} , Ca^{2+} , NO_3^- , Na^+ , with values respectively ranging from 0.20
867 to 0.96 $\text{kg ha}^{-1}\text{month}^{-1}$, from 0.13 to 3.84 $\text{kg. ha}^{-1}\text{month}^{-1}$, from 0.14 to 6.33 $\text{kg ha}^{-1}\text{month}^{-1}$, from 0.07 to
868 3.12 $\text{kg ha}^{-1}\text{month}^{-1}$ and from 0.07 to 4.38 $\text{kg ha}^{-1}\text{month}^{-1}$ (Figure 8).

869 Lamto displays dominant monthly wet deposition fluxes in decreasing order HCOO^- , NO_3^- , NH_4^+ , CH_3COO^-
870 and Ca^{2+} with values respectively range from 0.02 to 1.99 $\text{kg ha}^{-1}\text{month}^{-1}$, from 0.05 to 1.20 $\text{kg ha}^{-1}\text{month}^{-1}$
871 $^{-1}$, from 0.02 to 3.10 $\text{kg ha}^{-1}\text{month}^{-1}$ from 0.03 to 1.57 $\text{kg ha}^{-1}\text{month}^{-1}$ and from 0.02 to 4.39 $\text{kg ha}^{-1}\text{month}^{-1}$
872 respectively. Korhogo presents the same dominant ions in term of monthly wet deposition as Lamto with a
873 similar decreasing order: HCOO^- , NO_3^- , CH_3COO^- , NH_4^+ , Ca^{2+} and monthly wet deposition values are
874 ranged from 0.00 to 2.18 $\text{kg ha}^{-1}\text{month}^{-1}$, from 0.07 to 2.15 $\text{kg ha}^{-1}\text{month}^{-1}$, from 0.01 to 1.69 $\text{kg ha}^{-1}\text{month}^{-1}$
875 $^{-1}$, from 0.01 to 1.49 $\text{kg ha}^{-1}\text{month}^{-1}$ and from 0.04 to 1.51 $\text{kg ha}^{-1}\text{month}^{-1}$, respectively.

876 3.2.1 Seasonal and monthly concentration variation in Abidjan 877

878 On the Abidjan site, seasonal variation of the chemical signature of rainwater during the study period is well
879 marked. During the long dry season from December to February, rainwater chemistry is dominated by Ca^{2+} ,
880 SO_4^{2-} , NH_4^+ ions with VWM concentration ranging from 31.60 to 81.67 $\mu\text{eq L}^{-1}$, from 19.6 to 49.54 $\mu\text{eq L}^{-1}$
881 $^{-1}$, and from 30.53 to 32.80 $\mu\text{eq L}^{-1}$ respectively. In the long-wet season from March to July the predominant
882 ions are Na^+ , Cl^- respectively ranging from 3.72 to 67.84 $\mu\text{eq. L}^{-1}$ and from 4.01 to 83.79 $\mu\text{eq. L}^{-1}$ (Figure
883 8-a). High concentrations during the dry season are due to dust particles coming from north east warm and
884 dry desert air masses (light blue and yellow cells) (Figure 5-b) and to gases emitted by biomass burning. In
885 the wet season, Abidjan is under the influence of warm and humid monsoon air masses rich in sea salt which
886 explain the strong VWM concentrations of marine ions (Figure 5-c). The short dry season at Abidjan (from
887 August to mid-September) records VWM Na^+ , Cl^- concentrations ranging from 12.56 to 187.69 $\mu\text{eq. L}^{-1}$



888 and from 16.84 to 166.47 $\mu\text{eq. L}^{-1}$ respectively, showing the influence of monsoon air masses. During this
889 short dry season, coastal upwelling leads to a cooling of surface sea water which prevents the formation of
890 rain clouds due to a decrease in evaporation rate. The continental zone most impacted by this phenomenon
891 is the southeast of Ghana and extends towards the middle-east of Côte d'Ivoire where Abidjan is situated
892 (Ali et al., 2011). Finally, the short-wet season is marked by both marine ions Na^+ and Cl^- with VWM
893 concentrations ranging from 9.86 to 38.57 $\mu\text{eq. L}^{-1}$, and from 12.11 to 77.76 $\mu\text{eq. L}^{-1}$ respectively. Alkaline
894 ions (Ca^{2+} , NH_4^+) VWM concentrations ranged from 10.60 to 100.21 $\mu\text{eq. L}^{-1}$ and from 13.52 to 53.30 $\mu\text{eq.}$
895 L^{-1} respectively, highlighting a period of source mixing that indicates the end of the short-wet season and
896 the beginning of the long dry season.

897 Monthly VWM concentrations of major ions in Abidjan rains are on average 2 times higher in the long dry
898 season (December to February) than in the long- wet season (March to July). In the short-dry season,
899 monthly VWM concentrations are 3 times higher than in the short-wet season. Results indicate for the study
900 period (2018-2020) that the rain from the two dry seasons' rains represent only 12% of the total annual
901 rainfall and contributes to approximately 46% of the total measured chemical composition of precipitation.

902 3.2.2 Seasonal and monthly concentration variation in Lamto

903
904 At Lamto, rainwater chemistry is dominated by high monthly VWM NH_4^+ concentrations ranging from 6.14
905 to 146.58 $\mu\text{eq. L}^{-1}$ throughout the study period. During the long dry season from December to February,
906 chemical composition of rainwater is dominated by NH_4^+ , Ca^{2+} , HCO_3^- and NO_3^- with VWM concentration
907 value ranging from 28.20 to 146.58 $\mu\text{eq. L}^{-1}$, from 12.58 to 108.14 $\mu\text{eq. L}^{-1}$, from 8.14 to 83.91 $\mu\text{eq. L}^{-1}$ and
908 from 18.02 to 72.20 $\mu\text{eq. L}^{-1}$ respectively. The long-wet season is characterized by the same dominant ions
909 However, the level concentration of marine ions is higher than in the dry season. The influence of
910 nitrogenous and organic species in the dry season in Côte d' Ivoire is related to periods of intense biomass
911 burning. Adon et al. (2010) reported maximum nitrogenous gases concentrations in West and central Africa
912 in the dry season months . Osohou et al. (2019) confirmed this result and show that nitrogenous compounds
913 at Lamto are washed out by rainfall during the seven following months (April–October), with higher wet
914 deposition at the end of the dry season and at the beginning of the wet season, due to increased rainfall
915 during that period, when there is a strong influence of biomass burning (Figure 8-e). Monthly mean CrIS
916 NH_3 and OMI NO_2 vertical column densities (VCDs) and MODIS burned area fraction from January 2018
917 to December 2020 confirm that the highest NH_3 and NO_2 concentrations are related to active emission
918 sources in the dry season at all sites, but especially in Lamto (Figure 9). At Lamto, the highest monthly NH_3
919 and NO_2 VCDs are associated with the highest monthly burned area fractions, with monthly means ranging
920 respectively from 2.42×10^{16} to 4.53×10^{17} molecules $\text{NH}_3 \text{ cm}^{-1}$, 1.32 to 12.91×10^{15} molecules $\text{NO}_2 \text{ cm}^{-2}$
921 and from 0.75 to 35.91% area burned, highlighting the importance of biomass burning source in Lamto
922 compared to the two studied urban sites. During the dry season, Lamto is also under the influence of



923 harmattan air masses loaded with dust, which may explain the level of VWM Ca^{2+} concentration (Figure 8-
924 a) (Figure A2).

925

926

927

928

929

930

931

932

933

934

935

936

937



938
939
940
941
942
943
944
945
946
947
948
949
950
951
952
953
954
955
956
957
958
959
960
961
962
963
964
965
966
967
968
969
970
971
972
973
974
975
976
977
978
979
980
981
982
983
984
985
986
987
988
989
990
991

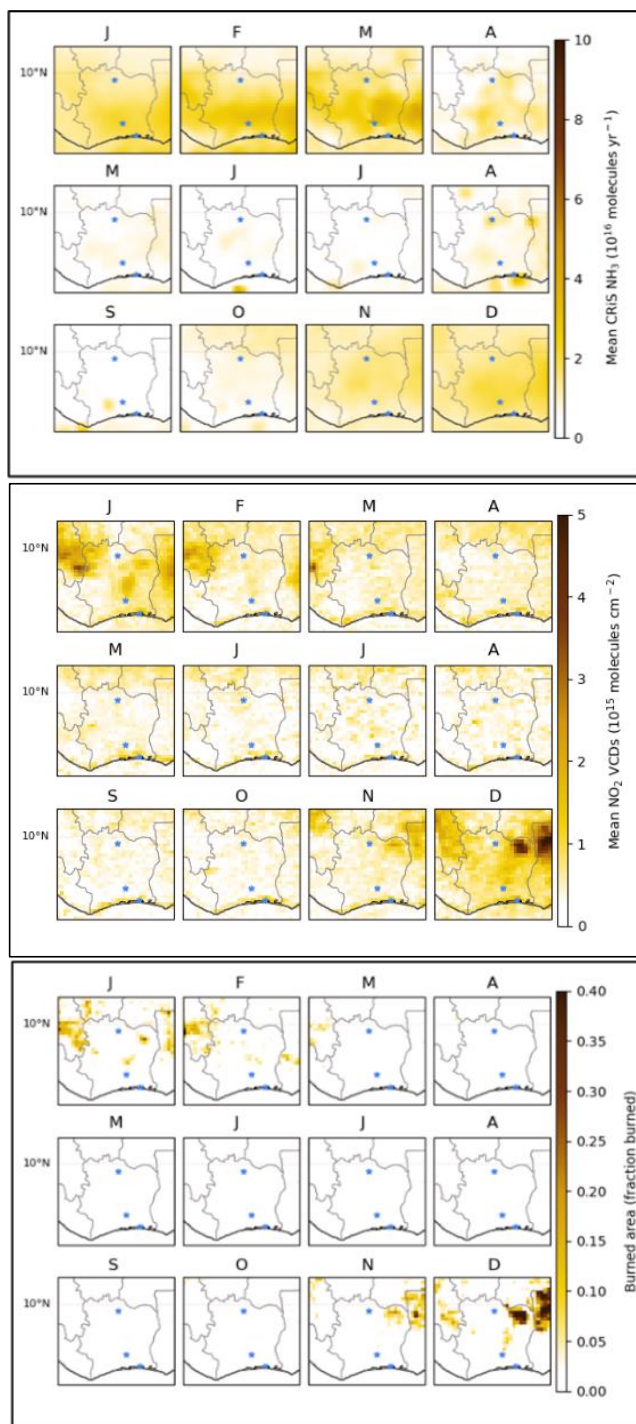


Figure 9: Monthly mean vertical column densities of NH_3 from CRiS (let panel), tropospheric vertical column densities of NO_2 from OMI (middle panel), and burned area from MODIS (right panel) averaged over 2018-2020. Note that the means for NH_3 do not include April-July 2019.



992 The marine ion and organic acid signature of the long-wet season is associated with the influence of oceanic
993 air masses on Lamto during the long-wet season (Figure 5-f). The short dry season restricted to August at
994 Lamto is significantly influenced by the marine source because of the same phenomenon described for the
995 short dry season in Abidjan. During the short-wet season from September to November, rainwater chemistry
996 is characterized by relatively high levels of concentrations of Ca^{2+} and NH_4^+ and with a signature of marine
997 ions and organic acids at the end of this season. In Lamto for the study period (2018-2020), monthly VWM
998 concentrations of major ions show that concentrations are on average 4 times higher in the long dry season
999 (December to February) than in the long-wet season (March to July) while concentrations in the short-dry
1000 season (August) are 3 times higher than in short-wet season (October to November). Rain from the dry
1001 seasons represent only 3 % of the total annual rainfall but approximately 74% of the total measured
1002 chemical composition of precipitation in Lamto

1003 3.2.3 Seasonal and monthly concentration variation in Korhogo

1004

1005 At Korhogo, the average seasonal evolution in Korhogo is marked by a predominance of Ca^{2+} , NO_3^- , SO_4^{2-}
1006 and NH_4^+ ions during the long dry season from November to March and a long-wet season from April to
1007 October, which presents rainwater chemical composition mainly dominated by the previously cited ions
1008 dominant in the long-dry season but with much lower VWM concentrations due to the dilution effect. In
1009 addition, in this long-wet season there is a signature of HCOO^- , Na^+ , and Cl^- ions in rains.

1010 Terrigenous compound abundance is related to the ITCZ position, which places Korhogo under the
1011 influence of dry and warm harmattan air masses. The high concentrations of nitrogenous compounds reflect
1012 on the one hand, the strong agricultural activity in the surroundings of the city as well as the use of fertilizer
1013 and biomass fires by farmers for field clearing before the wet season and on the other hand the relative
1014 importance of traffic source in NO_2 emissions from motorized vehicles. Satellite data analysis show that
1015 nitrogenous species reach their highest VCDs values in March-April at the end of the dry season at Korhogo;
1016 values ranged respectively from 2.74×10^{16} to 2.14×10^{17} molecules $\text{NH}_3 \text{ cm}^{-1}$, from 2.00 to 8.54×10^{15}
1017 molecules $\text{NO}_2 \cdot \text{cm}^{-2}$ and from 0.11 to 2.68% of burned area. The relative importance of SO_2 in dry seasons
1018 is likely to be related to biomass burning (burning of forest, grassland, and agricultural wastes), which could
1019 be also a significant source of SO_2 to the atmosphere which is more active in dry season than in wet
1020 season (Bates et al., 1992; Arndt et al., 1997).

1021 The increase in soil moisture at the beginning of the wet season is correlated to the increase of NO and NH_3
1022 concentrations in the dry savanna (Adon et al., 2010) and could explain a significant part of NH_4^+ and NO_3^-
1023 concentration at Korhogo. The growing vegetation in the wet season produces biogenic VOC emissions
1024 which are an important source of organic acids, and can explain the preponderance of HCOO^- in the wet
1025 season at Korhogo, similarly to the result observed in Lamto. (Niu et al., 2018) found similar results in



1026 China with highest acid concentrations in rains during the growing season (wet season) than in the non-
1027 growing seasons (dry season). Finally for the study period (2018-2020) in Korhogo, monthly VWM
1028 concentrations of major ions show that concentrations are on average 3 times higher in the long dry season
1029 (November to March) than in the long-wet season (April to October). The dry season's rains represent only
1030 3 % of the total annual rainfall, but approximatively 82% of the total measured chemical composition of
1031 precipitation in Korhogo.

1032

1033 4. Conclusion

1034 This paper documents rain chemical composition and associated wet deposition of major ionic species along
1035 a North-South transect in Côte d'Ivoire. This study presents original results over a three-year time period at
1036 two urban sites (Abidjan and Korhogo) inter-compared with a rural wet savanna site (Lamto) in Côte
1037 d'Ivoire. The mean precipitation chemical content and wet deposition fluxes are computed at the annual
1038 (2019 and 2020) and at the monthly scale for the full studied period (2018-2020). The dominant ion at both
1039 urban sites is Ca^{2+} , whereas NH_4^+ dominates the chemical content of the Lamto rural site. At Abidjan and
1040 Korhogo, Ca^{2+} , Na^+ , Cl^- , and NH_4^+ and Ca^{2+} , NH_4^+ , Na^+ , and HCOO^- , respectively dominate the total
1041 chemical content and represent 62% and 63% of the total. The rainwater chemical signature at the rural site
1042 of Lamto is dominated by NH_4^+ , HCOO^- , Ca^{2+} , and NO_3^- ions, representing 55 % of the total. The two urban
1043 sites of Abidjan and Korhogo rains are characterized by a terrigenous contribution associated to a mixture
1044 of terrigenous continental and anthropogenic sources respectively 39% and 33%, also a high marine
1045 contribution respectively 34 % and 24% and a significant nitrogenous contribution respectively 18 % and
1046 25 % mainly associated to fossil fuel from road traffic, domestic and biomass burning sources. At the rural
1047 Lamto site, marine, terrigenous and nitrogenous contribution represent respectively 14%, 25% and 30%. In
1048 addition to the high nitrogenous contribution related to biomass burning and agricultural sources, the site
1049 shows a strong organic component (23%) comparable to the one of Korhogo (16%). This original result has
1050 been associated to volatile organic compounds emissions from biomass burning and vegetation at the rural
1051 site and from domestic and landfill fires and traffic at the urban sites. Mean measured pH are respectively
1052 5.76, 5.31, and 5.54 for Abidjan, Lamto and Korhogo indicating the importance of neutralization processes
1053 in urban rainwater chemistry. Considering the eutrophication of the environment through rainwater,
1054 significant wet deposition fluxes of nitrogen have been measured and equal respectively $7.01 \text{ kgN}\cdot\text{ha}^{-1}\cdot\text{yr}^{-1}$,
1055 $4.61 \text{ kgN}\cdot\text{ha}^{-1}\cdot\text{yr}^{-1}$, $4.18 \text{ kgN}\cdot\text{ha}^{-1}\cdot\text{yr}^{-1}$ in Abidjan, Lamto and Korhogo. This unique study on rainfall
1056 composition in urban sites represents a first step to characterize urban deposition fluxes and to understand
1057 the composition of the atmosphere and the pollution levels in African cities. Quantifying urban key
1058 deposition species such nitrogen is important for closing the gap in regional budgets of ionic species, which
1059 are necessary for policy makers to manage atmospheric inputs to and outputs from local ecosystems,
1060 assuming that a portion of total emitted urban compounds are transported out of the city into the surrounding



1061 region. However, it is important to note that wet deposition studies should be complemented by dry
1062 deposition processes evaluation to assess the global deposition budgets to improve knowledge on the
1063 biogeochemical cycle balance, soil quality, water quality, and to improve global deposition models. There
1064 is a clear need for more long term, quality-controlled in situ measurements in African urban areas, Africa
1065 being a key continent in the future considering climate and environmental issues where national and
1066 international pollutants reduction directives should be taken.



1067

1068 Appendices

1069

1070

Species	ABIDJAN						LAMTO						KORHOGO					
	2019		2020		2019-2020		2019		2020		2019-2020		2019		2020		2019-2020	
	VWM	WD	VWM	WD	VWM	WD	VWM	WD	VWM	WD	VWM	WD	VWM	WD	VWM	WD	VWM	WD
H ⁺	4.00	0.05	4.14	0.07	4.1(±0.09)	0.06(±0.01)	6.54	0.10	6.62	0.07	6.57(±0.06)	0.09(±0.02)	2.59	0.03	5.65	0.06	4.09(±2.16)	0.05(±0.02)
pH	5.57		5.89		5.76		5.24		5.38		5.31		5.70		5.40		5.57	
Na ⁺	19	5.93	30.95	11.34	26(±8.43)	8.8(±3.82)	4.46	1.55	6.82	1.73	5.41(±1.67)	1.62(±0.13)	16.65	4.45	2.40	0.60	11.24(±10.08)	3(±2.83)
NH ₄ ⁺	25.19	6.16	20.7	5.94	22.6(±3.18)	6(±0.15)	16.47	4.48	20.01	3.97	17.9(±2.50)	4.20(±0.36)	18.40	3.86	16.55	3.23	17.38(±1.31)	3.50(±0.54)
N in NH ₄ ⁺	19.64	4.8	16.14	4.63	17.63	4.68	12.84	3.49	15.6	3.09	13.96	3.27	14.35	3.01	12.90	2.51	13.55	2.73
K ⁺	3.78	2	5.09	3.17	4.5(±0.93)	2.62(±0.83)	1.80	1.06	2.8	0.99	2(±0.35)	1.02(±0.05)	12.43	5.65	2.06	0.87	8.63(±7.34)	3.80(±3.52)
Ca ²⁺	24.19	6.57	48.35	15.44	38.3(±17.08)	11.32(±6.27)	7.93	2.40	12.85	2.84	9.91(±3.48)	2.59(±0.31)	24.08	5.61	13.27	2.88	20.09(±7.64)	4.50(±2.07)
Mg ²⁺	5.49	0.9	8.74	1.67	7.4(±2.30)	1.31(±0.55)	2.19	0.40	3.12	0.42	2.57(±0.65)	0.40(±0.01)	4.07	0.57	2.35	0.31	3.4(±1.21)	0.50(±0.20)
NO ₃ ⁻	8.79	7.39	12.77	12.62	11.1(±2.81)	10.16(±3.70)	6.26	5.86	8.63	5.89	7.22(±1.67)	5.84(±0.03)	10.72	7.73	6.97	4.68	9.09(±2.65)	6.30(±2.34)
N in NO ₃ ⁻	2.02	1.69	2.93	2.90	2.55	2.33	1.43	1.34	1.98	1.35	1.66	1.34	2.46	1.77	1.60	1.07	2.09	1.45
Cl ⁻	24.40	11.74	37.44	21.18	32(±9.22)	16.77(±6.68)	4.76	2.55	7.27	2.84	5.77(±1.77)	2.67(±0.21)	13.71	5.66	2.44	0.94	9.57(±7.94)	3.80(±3.48)
SO ₄ ²⁻	19.49	12.69	19.38	14.83	19.5(±0.08)	13.76(±1.52)	4.24	3.07	5.54	2.93	4.76(±0.92)	2.99(±0.10)	6.01	3.35	3.84	2.00	5.27(±1.53)	2.80(±1.04)
S in SO ₄ ²⁻	6.43	4.18	6.39	4.89	6.43	4.5	1.39	1.01	1.82	0.96	1.57	0.98	1.98	1.10	1.26	0.66	1.73	0.92
*tCarb	7.17	2.99	17.04	16.57	12(±4.01)	11(±5.51)	2.29	1.73	3.50	1.93	2.78(±0.80)	2.21(±0.64)	5.17	0.06	2.52	0.67	4.54(±1.87)	3.10(±0.19)
HCOO ⁻	5.57	3.48	7.76	5.70	6.80(±1.55)	4.65(±1.57)	9.74	6.76	14.12	7.16	11.51(±3.10)	6.91(±0.28)	8.71	4.66	11.18	5.57	9.97(±1.75)	5.20(±0.53)
CH ₃ COO ⁻	3.21	2.57	6.72	6.33	5.30(±2.48)	4.57(±2.66)	5.40	4.81	8.47	5.51	6.64(±2.17)	5.11(±0.49)	5.16	3.54	5.51	3.52	5.61(±0.24)	3.70(±0.10)
C ₂ H ₅ COO ⁻	0.00	0.00	0.00	0.00	0.00	0.00	0.08	0.00	0.14	0.00	0.10(±0.04)	0.00(±0.00)	0.00	0.00	0.00	0.00	0.00	0.00
C ₂ O ₄ ²⁻	4.08	1.69	1.28	1.83	1.4(±0.24)	1.89(±0.60)	0.94	0.64	1.41	0.70	1.13(±0.33)	1.33(±0.04)	3.09	1.62	0.48	0.39	2.09(±1.85)	1.10(±0.19)

1071

1072 Table A1: Annual Volume Weight Mean (VWM) ($\mu\text{eq L}^{-1}$) and wet deposition fluxes (WD) ($\text{KgX.ha}^{-1} \cdot \text{yr}^{-1}$) in
 1073 rainwater in Abidjan, Lamto and Korhogo, (Côte d' Ivoire).

1074

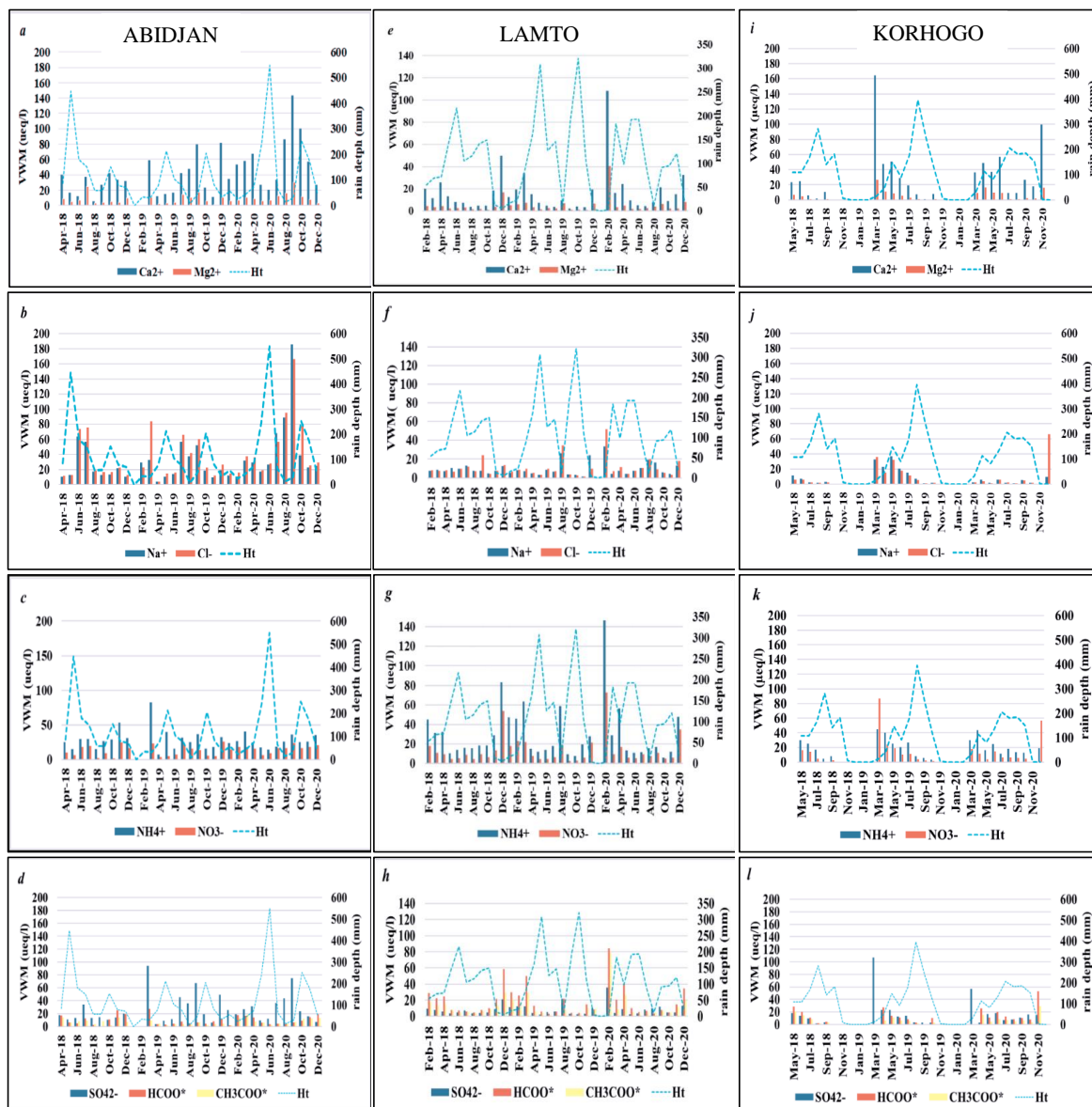
1075

1076

1077



1078



1079

1080 Figure A2: Monthly VWM ($\mu\text{eq. L}^{-1}$) variation of major ions in rainwater at Abidjan (a, b, c, d); Lamto (e, f,
 1081 g, h) Korhogo (I,j,k,l)

1082

1083

1084



Acronyms	Signification
AII	Annual Inter- variability Index
AP	Acidification Potential
EC	Electrical Conductivity
EF	Enrichment Factor
FA	Fractional Acidity
GAW	Global Atmospheric Watch
NF	Neutralization Factor
NP	Neutralization Potential
NSSF	Non-Sea salt Fraction
OMI	Ozone monitoring Instrument
pA	Potential Acidity
PC	Percentage Coverage
Pc	Precipitation Collected
PCL	Percentage Coverage Length
Pt	Annual Precipitation
SSF	Sea-Salt Fraction
VCD	Volume Column Density
WD	Wet Deposition
VWM	Volume Weighted Mean
WMO	World Meteorological Organization

1085

1086

TABLE A3: List of acronyms

1087 Data availability

1088 Raw data were collected in the framework of the PASMU project and are available on request from the
 1089 coordinator Pr V. Yoboué (yobouev@hotmail.com). Data of the LAMTO site are available from the
 1090 INDAAF project at the address <http://indaaf.obs-mip.fr> The pre-processed HYSPLIT trajectory data can
 1091 be obtained from the corresponding author, and the trajectories can be freely calculated at the web
 1092 page https://www.ready.noaa.gov/HYSPLIT_traj.php. MODIS burned-area data are available from
 1093 <https://doi.org/10.5067/MODIS/MCD64A1.006> (Giglio et al., 2015). OMI L3 NO SP version 4 is
 1094 available at [10.5067/MEASURES/MINDS/DATA301](https://doi.org/10.5067/MEASURES/MINDS/DATA301) (Lamsal et al., 2014). The CrIS CFPR version 1.6.3
 1095 NH3 VCD data is available upon request from Environment and Climate Change Canada
 1096 (mark.shephard@ec.gc.ca) https://hpfx.collab.science.gc.ca/~mas001/satellite_ext/cris/snpp/nh3/v1_6_3/
 1097 (Shephard et al., 2020).

1098

1099 Competing interests

1100 The authors declare that they have no conflict of interest

1101 Acknowledgements

1102 This work carried out in part within the framework of the PASMU project, financed by the Ministry of
 1103 Higher Education and Research of Côte d'Ivoire, in the framework of Debt Reduction-Development
 1104 Contracts (C2D) managed by the Research Institute for Development (IRD) under funding program
 1105 5768A1-PRO/PRESED-CI C2D PASMU project whose main agreement is registered under number



1106 305984/00. This work also received a contribution from the INDAAF program, supported by the
1107 INSU/CNRS, the IRD (Institut de Recherche pour le Développement), from the Observatoire des Sciences
1108 de l'Univers EFLUVE, from the Observatoire Midi-Pyrénées and the European Union's Horizon 2020
1109 research and innovation program under Marie Skłodowska-Curie grant agreement No. 871944. The
1110 authors would like to thank the PI and staff of the Lamto station in Côte d'Ivoire, SODEXAM (Airport,
1111 Aeronautical and Meteorological Development and Exploitation Company), EVIDENCE project (Extreme
1112 rainfall events, vulnerability to flooding and to water contamination) and finally the managers of the urban
1113 site located at the IRD within the FELIX HOUPHOUET BOIGNY University in (Abidjan) and the second
1114 urban site located at the PELOFORO GON COULIBALY University (Korhogo). We thank also Enrico
1115 Dammers and Mark Shephard for their assistance with CrIS NH₃ data.

1116

1117 References

- 1118 Adon, M., Galy-Lacaux, C., Yoboué, V., Delon, C., Lacaux, J. P., Castera, P., Gardrat, E., Pienaar, J., Al
1119 Ourabi, H., Laouali, D., Diop, B., Sigha-Nkamdjou, L., Akpo, A., Tathy, J. P., Lavenu, F., and Mougín,
1120 E.: Long term measurements of sulfur dioxide, nitrogen dioxide, ammonia, nitric acid and ozone in
1121 Africa using passive samplers, *Atmospheric Chem. Phys.*, 10, 7467–7487, [https://doi.org/10.5194/acp-](https://doi.org/10.5194/acp-10-7467-2010)
1122 10-7467-2010, 2010.
- 1123 Akpo, A. B., Galy-Lacaux, C., Laouali, D., Delon, C., Lioussé, C., Adon, M., Gardrat, E., Mariscal, A.,
1124 and Darakpa, C.: Precipitation chemistry and wet deposition in a remote wet savanna site in West Africa:
1125 Djougou (Benin), *Atmos. Environ.*, 115, 110–123, <https://doi.org/10.1016/j.atmosenv.2015.04.064>,
1126 2015.
- 1127 Ali, K. E., Kouadio, K. Y., Zahiri, E.-P., Aman, A., Assamoi, A. P., and Bourles, B.: Influence of the
1128 Gulf of Guinea Coastal and Equatorial Upwellings on the Precipitations along its Northern Coasts during
1129 the Boreal Summer Period, *Asian J. Appl. Sci.*, 4, 271–285, <https://doi.org/10.3923/ajaps.2011.271.285>,
1130 2011.
- 1131 Andreae, M. O., Andreae, T. W., Annegarn, H., Beer, J., Cachier, H., Le Canut, P., Elbert, W.,
1132 Maenhaut, W., Salma, I., Wienhold, F. G., and Zenker, T.: Airborne studies of aerosol emissions from
1133 savanna fires in southern Africa: 2. Aerosol chemical composition, *J. Geophys. Res. Atmospheres*, 103,
1134 32119–32128, <https://doi.org/10.1029/98JD02280>, 1998.
- 1135 Arndt, R. L., Carmichael, G. R., Streets, D. G., and Bhatti, N.: Sulfur dioxide emissions and sectorial
1136 contributions to sulfur deposition in Asia, *Atmos. Environ.*, 31, 1553–1572,
1137 [https://doi.org/10.1016/S1352-2310\(96\)00236-1](https://doi.org/10.1016/S1352-2310(96)00236-1), 1997.
- 1138 Avila, A., Queralt-Mitjans, I., and Alarcón, M.: Mineralogical composition of African dust delivered by
1139 red rains over northeastern Spain, *J. Geophys. Res. Atmospheres*, 102, 21977–21996,
1140 <https://doi.org/10.1029/97JD00485>, 1997.
- 1141 Bahino, J., Yoboué, V., Galy-Lacaux, C., Adon, M., Akpo, A., Keita, S., Lioussé, C., Gardrat, E.,
1142 Chiron, C., Osohou, M., Gnamien, S., and Djossou, J.: A pilot study of gaseous pollutants'



- 1143 measurement (NO₂, SO₂, NH₃, HNO₃ and O₃) in Abidjan, Côte d'Ivoire: contribution to an overview of
1144 gaseous pollution in African cities, *Atmospheric Chem. Phys.*, 18, 5173–5198,
1145 <https://doi.org/10.5194/acp-18-5173-2018>, 2018.
- 1146 Balasubramanian, R., Victor, T., and Chun, N.: [No title found], *Water. Air. Soil Pollut.*, 130, 451–456,
1147 <https://doi.org/10.1023/A:1013801805621>, 2001.
- 1148 Bassett, T. J.: Le boom de l'anacarde dans le bassin cotonnier du Nord ivoirien: Structures de marché et
1149 prix à la production, *Afr. Contemp.*, N° 263-264, 59–83, <https://doi.org/10.3917/afco.263.0059>, 2018.
- 1150 Bates, T. S., Lamb, B. K., Guenther, A., Dignon, J., and Stoiber, R. E.: Sulfur emissions to the
1151 atmosphere from natural sources, *J. Atmospheric Chem.*, 14, 315–337,
1152 <https://doi.org/10.1007/BF00115242>, 1992.
- 1153 Bobbink, R., Hicks, K., Galloway, J., Spranger, T., Alkemade, R., Ashmore, M., Bustamante, M.,
1154 Cinderby, S., Davidson, E., Dentener, F., Emmett, B., Erisman, J.-W., Fenn, M., Gilliam, F., Nordin, A.,
1155 Pardo, L., and De Vries, W.: Global assessment of nitrogen deposition effects on terrestrial plant
1156 diversity: a synthesis, *Ecol. Appl.*, 20, 30–59, <https://doi.org/10.1890/08-1140.1>, 2010.
- 1157 Cao, Y.-Z., Wang, S., Zhang, G., Luo, J., and Lu, S.: Chemical characteristics of wet precipitation at an
1158 urban site of Guangzhou, South China, *Atmospheric Res.*, 94, 462–469,
1159 <https://doi.org/10.1016/j.atmosres.2009.07.004>, 2009.
- 1160 Celle-Jeanton, H., Travi, Y., Loÿe-Pilot, M.-D., Huneau, F., and Bertrand, G.: Rainwater chemistry at a
1161 Mediterranean inland station (Avignon, France): Local contribution versus long-range supply,
1162 *Atmospheric Res.*, 91, 118–126, <https://doi.org/10.1016/j.atmosres.2008.06.003>, 2009.
- 1163 Chao, C. Y. and Wong, K. K.: Residential indoor PM₁₀ and PM_{2.5} in Hong Kong and the elemental
1164 composition, *Atmos. Environ.*, 36, 265–277, [https://doi.org/10.1016/S1352-2310\(01\)00411-3](https://doi.org/10.1016/S1352-2310(01)00411-3), 2002.
- 1165 Charlson, R. J. and Rodhe, H.: Factors controlling the acidity of natural rainwater, *Nature*, 295, 683–685,
1166 <https://doi.org/10.1038/295683a0>, 1982.
- 1167 Conradie, E. H., Van Zyl, P. G., Pienaar, J. J., Beukes, J. P., Galy-Lacaux, C., Venter, A. D., and
1168 Mkhathshwa, G. V.: The chemical composition and fluxes of atmospheric wet deposition at four sites in
1169 South Africa, *Atmos. Environ.*, 146, 113–131, <https://doi.org/10.1016/j.atmosenv.2016.07.033>, 2016.
- 1170 Dammers, E., Shephard, M. W., Palm, M., Cady-Pereira, K., Capps, S., Lutsch, E., Strong, K.,
1171 Hannigan, J. W., Ortega, I., Toon, G. C., Stremme, W., Grutter, M., Jones, N., Smale, D., Siemons, J.,
1172 Hrpcek, K., Tremblay, D., Schaap, M., Notholt, J., and Erisman, J. W.: Validation of the CrIS fast
1173 physical NH₃; retrieval with ground-based FTIR, *Atmospheric Meas. Tech.*, 10, 2645–2667,
1174 <https://doi.org/10.5194/amt-10-2645-2017>, 2017.
- 1175 Delmas, R., Lacaux, J. P., Menaut, J. C., Abbadie, L., Le Roux, X., Helas, G., and Lobert, J.: Nitrogen
1176 compound emission from biomass burning in tropical African savanna FOS/DECAFE 1991 experiment
1177 (Lamto, Ivory Coast), *J. Atmospheric Chem.*, 22, 175–193, <https://doi.org/10.1007/BF00708188>, 1995.
- 1178 Dentener, F. J. and Crutzen, P. J.: A three-dimensional model of the global ammonia cycle, *J.*
1179 *Atmospheric Chem.*, 19, 331–369, <https://doi.org/10.1007/BF00694492>, 1994.
- 1180 Diawara, A., Yoroba, F., Kouadio, K. Y., Kouassi, K. B., Assamoi, E. M., Diedhiou, A., and Assamoi,
1181 P.: Climate Variability in the Sudano-Guinean Transition Area and Its Impact on Vegetation: The Case



- 1182 of the Lamto Region in Côte D'Ivoire, *Adv. Meteorol.*, 2014, 1–11,
1183 <https://doi.org/10.1155/2014/831414>, 2014.
- 1184 Dominutti, P., Keita, S., Bahino, J., Colomb, A., Lioussé, C., Yoboué, V., Galy-Lacaux, C., Morris, E.,
1185 Bouvier, L., Sauvage, S., and Borbon, A.: Anthropogenic VOCs in Abidjan, southern West Africa: from
1186 source quantification to atmospheric impacts, *Atmospheric Chem. Phys.*, 19, 11721–11741,
1187 <https://doi.org/10.5194/acp-19-11721-2019>, 2019.
- 1188 Draxler, Roland. R. and Hess, G. D.: DESCRIPTION OF THE HYSPLIT_4 MODELING SYSTEM,
1189 1997.
- 1190 Drever, J. I.: *The geochemistry of natural waters: surface and groundwater environments*, 3rd ed.,
1191 Prentice Hall, Upper Saddle River, N.J, 436 pp., 1997.
- 1192 Ehrnsperger, L. and Klemm, O.: Source Apportionment of Urban Ammonia and its Contribution to
1193 Secondary Particle Formation in a Mid-size European City, *Aerosol Air Qual. Res.*, 21, 200404,
1194 <https://doi.org/10.4209/aaqr.2020.07.0404>, 2021.
- 1195 Fall, M. and Coulibaly, S. (Eds.): *L'Urbanisation diversifiée: Le cas de la Côte d'Ivoire*, The World
1196 Bank, <https://doi.org/10.1596/978-1-4648-0869-2>, 2016.
- 1197 Fernandes, A. M.: Características hidrogeoquímicas da bacia de drenagem do rio Sorocaba, SP:
1198 processos erosivos mecânicos e químicos, Doutorado em Química na Agricultura e no Ambiente,
1199 Universidade de São Paulo, Piracicaba, <https://doi.org/10.11606/T.64.2012.tde-26092012-165330>, 2012.
- 1200 Fowler, D., Coyle, M., Skiba, U., Sutton, M. A., Cape, J. N., Reis, S., Sheppard, L. J., Jenkins, A.,
1201 Grizzetti, B., Galloway, J. N., Vitousek, P., Leach, A., Bouwman, A. F., Butterbach-Bahl, K., Dentener,
1202 F., Stevenson, D., Amann, M., and Voss, M.: The global nitrogen cycle in the twenty-first century,
1203 *Philos. Trans. R. Soc. B Biol. Sci.*, 368, 20130164, <https://doi.org/10.1098/rstb.2013.0164>, 2013.
- 1204 Fu, Y., Li, F., Guo, S., and Zhao, M.: Cadmium concentration and its typical input and output fluxes in
1205 agricultural soil downstream of a heavy metal sewage irrigation area, *J. Hazard. Mater.*, 412, 125203,
1206 <https://doi.org/10.1016/j.jhazmat.2021.125203>, 2021.
- 1207 Galloway, J. N., Likens, G. E., Keene, W. C., and Miller, J. M.: The composition of precipitation in
1208 remote areas of the world, *J. Geophys. Res.*, 87, 8771, <https://doi.org/10.1029/JC087iC11p08771>, 1982.
- 1209 Galy-Lacaux, C. and Modi, A. I.: Precipitation Chemistry in the Sahelian Savanna of Niger, Africa., *J.*
1210 *Atmospheric Chem.*, 30, 319–343, <https://doi.org/10.1023/A:1006027730377>, 1998.
- 1211 Galy-Lacaux, C., Laouali, D., Descroix, L., Gobron, N., and Lioussé, C.: Long term precipitation
1212 chemistry and wet deposition in a remote dry savanna site in Africa (Niger), *Atmospheric Chem. Phys.*,
1213 9, 1579–1595, <https://doi.org/10.5194/acp-9-1579-2009>, 2009.
- 1214 Gao, Y., Zhou, F., Ciais, P., Miao, C., Yang, T., Jia, Y., Zhou, X., Klaus, B.-B., Yang, T., and Yu, G.:
1215 Human activities aggravate nitrogen-deposition pollution to inland water over China, *Natl. Sci. Rev.*, 7,
1216 430–440, <https://doi.org/10.1093/nsr/nwz073>, 2020.
- 1217 Gautier, L.: Contact forêt-savane en Côte d'Ivoire centrale : évolution de la surface forestière de la
1218 réserve de Lamto (sud du V-Baoulé.) *Candoella*, 45, 627–641, 1990.



- 1219 Gnamien, S., Yoboué, V., Liousse, C., Ossohou, M., Keita, S., Bahino, J., Siélé, S., and Diaby, L.:
1220 Particulate Pollution in Korhogo and Abidjan (Cote d'Ivoire) during the Dry Season, *Aerosol Air Qual.*
1221 *Res.*, 21, 200201, <https://doi.org/10.4209/aaqr.2020.05.0201>, 2021.
- 1222 Goula, B. T. A., SROHOUROU, B., BRIDA, A. B., KANGA, B. I., N'ZUÉ, K. A., and GOROZA, G.:
1223 Zoning of rainfall in Côte d'Ivoire, , November, 2010.
- 1224 Guenther, A.: Biological and Chemical Diversity of Biogenic Volatile Organic Emissions into the
1225 Atmosphere, *ISRN Atmospheric Sci.*, 2013, 1–27, <https://doi.org/10.1155/2013/786290>, 2013.
- 1226 Guenther, A., Karl, T., Harley, P., Wiedinmyer, C., Palmer, P. I., and Geron, C.: Estimates of global
1227 terrestrial isoprene emissions using MEGAN (Model of Emissions of Gases and Aerosols from Nature),
1228 *Atmospheric Chem. Phys.*, 6, 3181–3210, <https://doi.org/10.5194/acp-6-3181-2006>, 2006.
- 1229 Güzel, B.: Monitoring of the Chemical Composition of Rainwater in a Semi-Urban Area in the Northern
1230 West of Turkey, *GAZI Univ. J. Sci.*, 1–1, <https://doi.org/10.35378/gujs.727114>, 2020.
- 1231 Hoinaski, L., Franco, D., Stuetz, R. M., Sivret, E. C., and de Melo Lisboa, H.: Investigation of PM₁₀
1232 sources in Santa Catarina, Brazil through graphical interpretation analysis combined with receptor
1233 modelling, *Environ. Technol.*, 34, 2453–2463, <https://doi.org/10.1080/21622515.2013.772659>, 2013.
- 1234 Hoinaski, L., Franco, D., Haas, R., Martins, R. F., and Lisboa, H. de M.: Investigation of rainwater
1235 contamination sources in the southern part of Brazil, *Environ. Technol.*, 35, 868–881,
1236 <https://doi.org/10.1080/09593330.2013.854412>, 2014.
- 1237 Huang, D.-Y., Xu, Y.-G., Peng, P., Zhang, H.-H., and Lan, J.-B.: Chemical composition and seasonal
1238 variation of acid deposition in Guangzhou, South China: Comparison with precipitation in other major
1239 Chinese cities, *Environ. Pollut.*, 157, 35–41, <https://doi.org/10.1016/j.envpol.2008.08.001>, 2009.
- 1240 INS, I. N. de S. de C. d' I.: RPGH2014, 2014.
- 1241 Josipovic, M., Annegarn, H. J., Kneen, M. A., Pienaar, J. J., and Piketh, S. J.: Atmospheric dry and wet
1242 deposition of sulphur and nitrogen species and assessment of critical loads of acidic deposition
1243 exceedance in South Africa, *South Afr. J. Sci.*, 107, 10 pages, <https://doi.org/10.4102/sajs.v107i3/4.478>,
1244 2011.
- 1245 Kaba, A. J.: Explaining Africa's Rapid Population Growth, 1950 to 2020: Trends, Factors, Implications,
1246 and Recommendations, *Sociol. Mind*, 10, 226–268, <https://doi.org/10.4236/sm.2020.104015>, 2020.
- 1247 Kaufman, Y. J.: Dust transport and deposition observed from the Terra-Moderate Resolution Imaging
1248 Spectroradiometer (MODIS) spacecraft over the Atlantic Ocean, *J. Geophys. Res.*, 110, D10S12,
1249 <https://doi.org/10.1029/2003JD004436>, 2005.
- 1250 Keene, W. C. and Galloway, J. N.: Considerations regarding sources for formic and acetic acids in the
1251 troposphere, *J. Geophys. Res.*, 91, 14466, <https://doi.org/10.1029/JD091iD13p14466>, 1986.
- 1252 Keene, W. C., Pszenny, A. A. P., Galloway, J. N., and Hawley, M. E.: Sea-salt corrections and
1253 interpretation of constituent ratios in marine precipitation, *J. Geophys. Res.*, 91, 6647,
1254 <https://doi.org/10.1029/JD091iD06p06647>, 1986.



- 1255 Keresztesi, Á., Birsan, M.-V., Nita, I.-A., Bodor, Z., and Szép, R.: Assessing the neutralisation, wet
1256 deposition and source contributions of the precipitation chemistry over Europe during 2000–2017,
1257 *Environ. Sci. Eur.*, 31, 50, <https://doi.org/10.1186/s12302-019-0234-9>, 2019.
- 1258 Keresztesi, Á., Nita, I.-A., Boga, R., Birsan, M.-V., Bodor, Z., and Szép, R.: Spatial and long-term
1259 analysis of rainwater chemistry over the conterminous United States, *Environ. Res.*, 188, 109872,
1260 <https://doi.org/10.1016/j.envres.2020.109872>, 2020.
- 1261 Kharol, S. K., Shephard, M. W., McLinden, C. A., Zhang, L., Sioris, C. E., O'Brien, J. M., Vet, R.,
1262 Cady-Pereira, K. E., Hare, E., Siemons, J., and Krotkov, N. A.: Dry Deposition of Reactive Nitrogen
1263 From Satellite Observations of Ammonia and Nitrogen Dioxide Over North America, *Geophys. Res.
1264 Lett.*, 45, 1157–1166, <https://doi.org/10.1002/2017GL075832>, 2018.
- 1265 Khwaja, H. A. and Husain, L.: Chemical characterization of acid precipitation in Albany, New York,
1266 *Atmospheric Environ. Part Gen. Top.*, 24, 1869–1882, [https://doi.org/10.1016/0960-1686\(90\)90519-S](https://doi.org/10.1016/0960-1686(90)90519-S),
1267 1990.
- 1268 Kouadio, Y. K., Ochou, D. A., and Servain, J.: Tropical Atlantic and rainfall variability in Côte d'Ivoire:
1269 ATLANTIC AND RAINFALL IN COTE D'IVOIRE, *Geophys. Res. Lett.*, 30, n/a-n/a,
1270 <https://doi.org/10.1029/2002GL015290>, 2003.
- 1271 Krotkov, N. A., Lamsal, L. N., Celarier, E. A., Swartz, W. H., Marchenko, S. V., Bucsel, E. J., Chan, K.
1272 L., and Wenig, M.: The version 3 OMI NO₂; standard product, *Gases/Remote Sensing/Data Processing
1273 and Information Retrieval*, <https://doi.org/10.5194/amt-2017-44>, 2017.
- 1274 Kulshrestha, U. C., Kulshrestha, M. J., Sekar, R., Sastry, G. S. R., and Vairamani, M.: Chemical
1275 characteristics of rainwater at an urban site of south-central India, *Atmos. Environ.*, 37, 3019–3026,
1276 [https://doi.org/10.1016/S1352-2310\(03\)00266-8](https://doi.org/10.1016/S1352-2310(03)00266-8), 2003.
- 1277 L Kok, PG van Zyl, JP Beukes, J-S Swartz, RP Burger, Suria Ellis, M Josipovic, V Vakkari, L Laakso,
1278 and M Kulmala: Chemical composition of rain at a regional site on the South African Highveld, *Water
1279 SA*, 47, <https://doi.org/10.17159/wsa/2021.v47.i3.11861>, 2021.
- 1280 Lamsal, L. N., Krotkov, N. A., Celarier, E. A., Swartz, W. H., Pickering, K. E., Bucsel, E. J., Gleason,
1281 J. F., Martin, R. V., Philip, S., Irie, H., Cede, A., Herman, J., Weinheimer, A., Szykman, J. J., and
1282 Knepp, T. N.: Evaluation of OMI operational standard NO₂; column retrievals using in situ and surface-
1283 based NO₂ observations, *Atmospheric Chem. Phys.*, 14, 11587–11609, [https://doi.org/10.5194/acp-14-
1284 11587-2014](https://doi.org/10.5194/acp-14-11587-2014), 2014.
- 1285 Laouali, D., Galy-Lacaux, C., Diop, B., Delon, C., Orange, D., Lacaux, J. P., Akpo, A., Lavenu, F.,
1286 Gardrat, E., and Castera, P.: Long term monitoring of the chemical composition of precipitation and wet
1287 deposition fluxes over three Sahelian savannas, *Atmos. Environ.*, 50, 314–327,
1288 <https://doi.org/10.1016/j.atmosenv.2011.12.004>, 2012.
- 1289 Laouali, D., Delon, C., Adon, M., Ndiaye, O., Saneh, I., Gardrat, E., Dias-Alves, M., Tagesson, T.,
1290 Fensholt, R., and Galy-Lacaux, C.: Source contributions in precipitation chemistry and analysis of
1291 atmospheric nitrogen deposition in a Sahelian dry savanna site in West Africa, *Atmospheric Res.*, 251,
1292 105423, <https://doi.org/10.1016/j.atmosres.2020.105423>, 2021.
- 1293 Lara, L. B. L. S., Artaxo, P., Martinelli, L. A., Victoria, R. L., Camargo, P. B., Krusche, A., Ayers, G. P.,
1294 Ferraz, E. S. B., and Ballester, M. V.: Chemical composition of rainwater and anthropogenic influences



- 1295 in the Piracicaba River Basin, Southeast Brazil, *Atmos. Environ.*, 35, 4937–4945,
1296 [https://doi.org/10.1016/S1352-2310\(01\)00198-4](https://doi.org/10.1016/S1352-2310(01)00198-4), 2001.
- 1297 Leroux, M.: The meteorology and climate of tropical Africa, Springer ; Praxis Pub, London ; New York :
1298 Chichester, UK, 548 pp., 2001.
- 1299 Li, C., Li, S.-L., Yue, F.-J., He, S.-N., Shi, Z.-B., Di, C.-L., and Liu, C.-Q.: Nitrate sources and
1300 formation of rainwater constrained by dual isotopes in Southeast Asia: Example from Singapore,
1301 *Chemosphere*, 241, 125024, <https://doi.org/10.1016/j.chemosphere.2019.125024>, 2020.
- 1302 Lu, X., Li, L. Y., Li, N., Yang, G., Luo, D., and Chen, J.: Chemical characteristics of spring rainwater of
1303 Xi'an city, NW China, *Atmos. Environ.*, 45, 5058–5063,
1304 <https://doi.org/10.1016/j.atmosenv.2011.06.026>, 2011.
- 1305 Marc, G., Marietta, H., Andreas, M., and Gian-Valentino, V.: Dirty diesel, *Public Eye*, September, 2016.
- 1306 Marticorena, B., Chatenet, B., Rajot, J. L., Traoré, S., Coulibaly, M., Diallo, A., Koné, I., Maman, A.,
1307 NDiaye, T., and Zakou, A.: Temporal variability of mineral dust concentrations over West Africa:
1308 analyses of a pluriannual monitoring from the AMMA Sahelian Dust Transect, *Atmospheric Chem.*
1309 *Phys.*, 10, 8899–8915, <https://doi.org/10.5194/acp-10-8899-2010>, 2010.
- 1310 Martins, E. H., Nogarotto, D. C., Mortatti, J., and Pozza, S. A.: Chemical composition of rainwater in an
1311 urban area of the southeast of Brazil, *Atmospheric Pollut. Res.*, 10, 520–530,
1312 <https://doi.org/10.1016/j.apr.2018.10.003>, 2019.
- 1313 McLinden, C. A., Fioletov, V., Boersma, K. F., Kharol, S. K., Krotkov, N., Lamsal, L., Makar, P. A.,
1314 Martin, R. V., Veeffkind, J. P., and Yang, K.: Improved satellite retrievals of NO₂; and SO₂; over the
1315 Canadian oil sands and comparisons with surface measurements, *Atmospheric Chem. Phys.*, 14, 3637–
1316 3656, <https://doi.org/10.5194/acp-14-3637-2014>, 2014.
- 1317 de Mello, W. Z.: Precipitation chemistry in the coast of the Metropolitan Region of Rio de Janeiro,
1318 Brazil, *Environ. Pollut.*, 114, 235–242, [https://doi.org/10.1016/S0269-7491\(00\)00209-8](https://doi.org/10.1016/S0269-7491(00)00209-8), 2001.
- 1319 Migliavacca, D., Teixeira, E., Wiegand, F., Machado, A., and Sanchez, J.: Atmospheric precipitation and
1320 chemical composition of an urban site, Guaba hydrographic basin, Brazil, *Atmos. Environ.*, 39, 1829–
1321 1844, <https://doi.org/10.1016/j.atmosenv.2004.12.005>, 2005.
- 1322 Moreda-Piñeiro, J., Alonso-Rodríguez, E., Moscoso-Pérez, C., Blanco-Heras, G., Turnes-Carou, I.,
1323 López-Mahía, P., Muniategui-Lorenzo, S., and Prada-Rodríguez, D.: Influence of marine, terrestrial and
1324 anthropogenic sources on ionic and metallic composition of rainwater at a suburban site (northwest coast
1325 of Spain), *Atmos. Environ.*, 88, 30–38, <https://doi.org/10.1016/j.atmosenv.2014.01.067>, 2014.
- 1326 Mphepya, J. N., Pienaar, J. J., Galy-Lacaux, C., Held, G., and Turner, C. R.: Precipitation Chemistry in
1327 Semi-Arid Areas of Southern Africa: A Case Study of a Rural and an Industrial Site, *J. Atmospheric*
1328 *Chem.*, 47, 1–24, <https://doi.org/10.1023/B:JOCH.0000012240.09119.c4>, 2004.
- 1329 Naimabadi, A., Shirmardi, M., Maleki, H., Teymouri, P., Goudarzi, G., Shahsavani, A., Sorooshian, A.,
1330 Babaei, A. A., Mehrabi, N., Baneshi, M. M., Zarei, M. R., Lababpour, A., and Ghozikali, M. G.: On the
1331 chemical nature of precipitation in a populated Middle Eastern Region (Ahvaz, Iran) with diverse
1332 sources, *Ecotoxicol. Environ. Saf.*, 163, 558–566, <https://doi.org/10.1016/j.ecoenv.2018.07.103>, 2018.



- 1333 Nicholson, S. E.: The West African Sahel: A Review of Recent Studies on the Rainfall Regime and Its
1334 Interannual Variability, *ISRN Meteorol.*, 2013, 1–32, <https://doi.org/10.1155/2013/453521>, 2013.
- 1335 Nilsson, J.: Critical Loads for Sulphur and Nitrogen, in: *Air Pollution and Ecosystems*, edited by: Mathy,
1336 P., Springer Netherlands, Dordrecht, 85–91, https://doi.org/10.1007/978-94-009-4003-1_11, 1988.
- 1337 Niu, H., He, Y., Zhu, G., Xin, H., Du, J., Pu, T., Lu, X., and Zhao, G.: Environmental implications of the
1338 snow chemistry from Mt. Yulong, southeastern Tibetan Plateau, *Quat. Int.*, 313–314, 168–178,
1339 <https://doi.org/10.1016/j.quaint.2012.11.019>, 2013.
- 1340 Niu, Y., Li, X., Pu, J., and Huang, Z.: Organic acids contribute to rainwater acidity at a rural site in
1341 eastern China, *Air Qual. Atmosphere Health*, 11, 459–469, <https://doi.org/10.1007/s11869-018-0553-9>,
1342 2018.
- 1343 Ossohou, M., Galy-Lacaux, C., Yoboué, V., Hickman, J. E., Gardrat, E., Adon, M., Darras, S., Laouali,
1344 D., Akpo, A., Ouafo, M., Diop, B., and Opepa, C.: Trends and seasonal variability of atmospheric NO₂
1345 and HNO₃ concentrations across three major African biomes inferred from long-term series of ground-
1346 based and satellite measurements, *Atmos. Environ.*, 207, 148–166,
1347 <https://doi.org/10.1016/j.atmosenv.2019.03.027>, 2019.
- 1348 Park, S.-M., Seo, B.-K., Lee, G., Kahng, S.-H., and Jang, Y.: Chemical Composition of Water Soluble
1349 Inorganic Species in Precipitation at Shihwa Basin, Korea, *Atmosphere*, 6, 732–750,
1350 <https://doi.org/10.3390/atmos6060732>, 2015.
- 1351 Payus, C. M., Jikilim, C., and Sentian, J.: Rainwater chemistry of acid precipitation occurrences due to
1352 long-range transboundary haze pollution and prolonged drought events during southwest monsoon
1353 season: climate change driven, *Heliyon*, 6, e04997, <https://doi.org/10.1016/j.heliyon.2020.e04997>, 2020.
- 1354 Possanzini, M., Buttini, P., and Di Palo, V.: Characterization of a rural area in terms of dry and wet
1355 deposition, *Sci. Total Environ.*, 74, 111–120, [https://doi.org/10.1016/0048-9697\(88\)90132-5](https://doi.org/10.1016/0048-9697(88)90132-5), 1988.
- 1356 Radojevic, M. and Harrison, R. M. (Eds.): *Atmospheric acidity: sources, consequences, and abatement*,
1357 Elsevier Applied Science, London ; New York, 587 pp., 1992.
- 1358 Rao, W., Han, G., Tan, H., Jin, K., Wang, S., and Chen, T.: Chemical and Sr isotopic characteristics of
1359 rainwater on the Alxa Desert Plateau, North China: Implication for air quality and ion sources,
1360 *Atmospheric Res.*, 193, 163–172, <https://doi.org/10.1016/j.atmosres.2017.04.007>, 2017.
- 1361 Rastogi, N. and Sarin, M.: Chemical characteristics of individual rain events from a semi-arid region in
1362 India: Three-year study, *Atmos. Environ.*, 39, 3313–3323,
1363 <https://doi.org/10.1016/j.atmosenv.2005.01.053>, 2005.
- 1364 Riccio, A., Chianese, E., Tirimberio, G., and Prati, M. V.: Emission factors of inorganic ions from road
1365 traffic: A case study from the city of Naples (Italy), *Transp. Res. Part Transp. Environ.*, 54, 239–249,
1366 <https://doi.org/10.1016/j.trd.2017.05.008>, 2017.
- 1367 Rockström, J., Steffen, W., Noone, K., Persson, Å., Chapin, F. S., Lambin, E. F., Lenton, T. M.,
1368 Scheffer, M., Folke, C., Schellnhuber, H. J., Nykvist, B., de Wit, C. A., Hughes, T., van der Leeuw, S.,
1369 Rodhe, H., Sörlin, S., Snyder, P. K., Costanza, R., Svedin, U., Falkenmark, M., Karlberg, L., Corell, R.
1370 W., Fabry, V. J., Hansen, J., Walker, B., Liverman, D., Richardson, K., Crutzen, P., and Foley, J. A.: A
1371 safe operating space for humanity, *Nature*, 461, 472–475, <https://doi.org/10.1038/461472a>, 2009.



- 1372 Roger, D. M., Abou, D., Denis, H. K., and Koffi, B. É.: Émergence De Taxi-Motos Et Recomposition
1373 SpatioÉconomique À Korhogo : Les Taxi-Villes Entre Stratégies D’adaptation Et Désespoir, Eur. Sci. J.
1374 ESJ, 12, 190, <https://doi.org/10.19044/esj.2016.v12n35p190>, 2016.
- 1375 Safai, P. D., Rao, P. S. P., Momin, G. A., Ali, K., Chate, D. M., and Praveen, P. S.: Chemical
1376 composition of precipitation during 1984–2002 at Pune, India, Atmos. Environ., 38, 1705–1714,
1377 <https://doi.org/10.1016/j.atmosenv.2003.12.016>, 2004.
- 1378 Samara, C. and Tsitouridou, R.: FINE AND COARSE IONIC AEROSOL COMPONENTS IN
1379 RELATION TO WET AND DRY DEPOSITION, Water. Air. Soil Pollut., 120, 71–88,
1380 <https://doi.org/10.1023/A:1005267021828>, 2000.
- 1381 Sangare, N., DOHO, B. T. andre, Kouakou, B., and Koffi, B. É.: Urban dynamics and governance of
1382 peri-urban neighbourhoods in the city of Korhogo (Côte d’Ivoire) from 2002 to 2020, EDUCI, 2021.
- 1383 Sarr, M. A.: Évolution récente du climat et de la végétation au Sénégal : cas du Bassin versant du Ferlo,
1384 Université Jean Moulin, Lyon, 2009.
- 1385 Schlesinger, WilliamH. and Hartley, AnneE.: A global budget for atmospheric NH₃, Biogeochemistry,
1386 15, <https://doi.org/10.1007/BF00002936>, 1992.
- 1387 Seinfeld, J. H.: Atmospheric chemistry and physics of air pollution, Wiley, New York, 738 pp., 1986.
- 1388 Seinfeld, J. H. and Pandis, S. N.: Atmospheric chemistry and physics: from air pollution to climate
1389 change, Wiley, New York, 1326 pp., 1998.
- 1390 Serça, D., Delmas, R., Le Roux, X., Parsons, D. A. B., Scholes, M. C., Abbadie, L., Lensi, R., Ronce, O.,
1391 and Labroue, L.: Comparison of nitrogen monoxide emissions from several African tropical ecosystems
1392 and influence of season and fire, Glob. Biogeochem. Cycles, 12, 637–651,
1393 <https://doi.org/10.1029/98GB02737>, 1998.
- 1394 Shakya, K. M., Peltier, R. E., Shrestha, H., and Byanju, R. M.: Measurements of TSP, PM₁₀, PM_{2.5},
1395 BC, and PM chemical composition from an urban residential location in Nepal, Atmospheric Pollut.
1396 Res., 8, 1123–1131, <https://doi.org/10.1016/j.apr.2017.05.002>, 2017.
- 1397 Shephard, M. W. and Cady-Pereira, K. E.: Cross-track Infrared Sounder (CrIS) satellite observations of
1398 tropospheric ammonia, Atmospheric Meas. Tech., 8, 1323–1336, [https://doi.org/10.5194/amt-8-1323-](https://doi.org/10.5194/amt-8-1323-2015)
1399 2015, 2015.
- 1400 Shephard, M. W., Dammers, E., Cady-Pereira, K. E., Kharol, S. K., Thompson, J., Gainariu-Matz, Y.,
1401 Zhang, J., McLinden, C. A., Kovachik, A., Moran, M., Bittman, S., Sioris, C. E., Griffin, D., Alvarado,
1402 M. J., Lonsdale, C., Savic-Jovcic, V., and Zheng, Q.: Ammonia measurements from space with the
1403 Cross-track Infrared Sounder: characteristics and applications, Atmospheric Chem. Phys., 20, 2277–
1404 2302, <https://doi.org/10.5194/acp-20-2277-2020>, 2020.
- 1405 Sigha-Nkamdjou, L., Galy-Lacaux, C., Pont, V., Richard, S., Sighomnou, D., and Lacaux, J. P.: [No title
1406 found], J. Atmospheric Chem., 46, 173–198, <https://doi.org/10.1023/A:1026057413640>, 2003a.
- 1407 Sigha-Nkamdjou, L., Galy-Lacaux, C., Pont, V., Richard, S., Sighomnou, D., and Lacaux, J. P.: [No title
1408 found], J. Atmospheric Chem., 46, 173–198, <https://doi.org/10.1023/A:1026057413640>, 2003b.



- 1409 Sun, X., Wang, Y., Li, H., Yang, X., Sun, L., Wang, X., Wang, T., and Wang, W.: Organic acids in
1410 cloud water and rainwater at a mountain site in acid rain areas of South China, *Environ. Sci. Pollut. Res.*,
1411 23, 9529–9539, <https://doi.org/10.1007/s11356-016-6038-1>, 2016.
- 1412 Suzanne, N. A.: Agriculture Traditionnelle Et Échecs Des Politiques De Gestion Des Aires Protégées En
1413 Côte d'Ivoire : Le Cas De La Réserve De Lamto, *Eur. Sci. J. ESJ*, 12, 209,
1414 <https://doi.org/10.19044/esj.2016.v12n30p209>, 2016.
- 1415 Tiwari, S., Kulshrestha, U. C., and Padmanabhamurty, B.: Monsoon rain chemistry and source
1416 apportionment using receptor modeling in and around National Capital Region (NCR) of Delhi, India,
1417 *Atmos. Environ.*, 41, 5595–5604, <https://doi.org/10.1016/j.atmosenv.2007.03.003>, 2007.
- 1418 Tiwari, S., Hopke, P. K., Thimmaiah, D., Dumka, U. C., Srivastava, A. K., Bisht, D. S., Rao, P. S. P.,
1419 Chate, D. M., Srivastava, M. K., and Tripathi, S. N.: Nature and Sources of Ionic Species in Precipitation
1420 across the Indo-Gangetic Plains, India, *Aerosol Air Qual. Res.*, 16, 943–957,
1421 <https://doi.org/10.4209/aaqr.2015.06.0423>, 2016.
- 1422 (UN World Urban Population: World Urbanization Prospects The 2011 Revision, 2011.
- 1423 United Nations, Department of Economic and Social Affairs, Population Division: World Population
1424 Prospects: The 2017 Revision, Key Findings and Advance Tables. Working Paper No. ESA/P/WP/248.,
1425 2017.
- 1426 Vet, R., Artz, R. S., Carou, S., Shaw, M., Ro, C.-U., Aas, W., Baker, A., Bowersox, V. C., Dentener, F.,
1427 Galy-Lacaux, C., Hou, A., Pienaar, J. J., Gillett, R., Forti, M. C., Gromov, S., Hara, H., Khodzher, T.,
1428 Mahowald, N. M., Nickovic, S., Rao, P. S. P., and Reid, N. W.: A global assessment of precipitation
1429 chemistry and deposition of sulfur, nitrogen, sea salt, base cations, organic acids, acidity and pH, and
1430 phosphorus, *Atmos. Environ.*, 93, 3–100, <https://doi.org/10.1016/j.atmosenv.2013.10.060>, 2014.
- 1431 Wai, K. M., Tanner, P. A., and Tam, C. W. F.: 2-Year Study of Chemical Composition of Bulk
1432 Deposition in a South China Coastal City: Comparison with East Asian Cities, *Environ. Sci. Technol.*,
1433 39, 6542–6547, <https://doi.org/10.1021/es048897d>, 2005.
- 1434 Wang, Y., Wai, K., Gao, J., Liu, X., Wang, T., and Wang, W.: The impacts of anthropogenic emissions
1435 on the precipitation chemistry at an elevated site in North-eastern China, *Atmos. Environ.*, 42, 2959–
1436 2970, <https://doi.org/10.1016/j.atmosenv.2007.12.051>, 2008.
- 1437 Whelpdale, D. M., Summers, P. W., and Sanhueza, E.: [No title found], *Environ. Monit. Assess.*, 48,
1438 217–247, <https://doi.org/10.1023/A:1005708821454>, 1997.
- 1439 WMO: WMO-GAW , ‘Manual for the GAW precipitation chemistry programme’, WMO TD No. 1251.,
1440 2004.
- 1441 World Bank: Towards Environmentally Sustainable Development in Sub-Saharan Africa. Africa Region
1442 Findings & Good Practice Infobriefs; No. 78. Washington, DC., 2017.
- 1443 World Meteorological Organization: State of the Climate in Africa, 2020, 2021.
- 1444 Xing, J., Song, J., Yuan, H., Li, X., Li, N., Duan, L., Qu, B., Wang, Q., and Kang, X.: Chemical
1445 characteristics, deposition fluxes and source apportionment of precipitation components in the Jiaozhou
1446 Bay, North China, *Atmospheric Res.*, 190, 10–20, <https://doi.org/10.1016/j.atmosres.2017.02.001>, 2017.



- 1447 Xu, Z., Wu, Y., Liu, W.-J., Liang, C.-S., Ji, J., Zhao, T., and Zhang, X.: Chemical composition of
1448 rainwater and the acid neutralizing effect at Beijing and Chizhou city, China, *Atmospheric Res.*, 164–
1449 165, 278–285, <https://doi.org/10.1016/j.atmosres.2015.05.009>, 2015.
- 1450 Yao, K. and Echui, A. désiré: RENOUELEMENT DU PARC AUTOMOBILE ET
1451 DEVELOPPEMENT DURABLE EN COTE D’IVOIRE, Conférence CODATU XVII - Mobilité
1452 Intelligente, Inclusive et Soutenable Hyderabad (Inde) -, inde, 2016.
- 1453 Yoboué, V., Galy-Lacaux, C., Lacaux, J. P., and Silué, S.: Rainwater Chemistry and Wet Deposition
1454 over the Wet Savanna Ecosystem of Lamto (Côte d’Ivoire), *J. Atmospheric Chem.*, 52, 117–141,
1455 <https://doi.org/10.1007/s10874-005-0281-z>, 2005a.
- 1456 Yoboué, V., Galy-Lacaux, C., Lacaux, J. P., and Silué, S.: Rainwater Chemistry and Wet Deposition
1457 over the Wet Savanna Ecosystem of Lamto (Côte d’Ivoire), *J. Atmospheric Chem.*, 52, 117–141,
1458 <https://doi.org/10.1007/s10874-005-0281-z>, 2005b.
- 1459 Zhang, M., Wang, S., Wu, F., Yuan, X., and Zhang, Y.: Chemical compositions of wet precipitation and
1460 anthropogenic influences at a developing urban site in southeastern China, *Atmospheric Res.*, 84, 311–
1461 322, <https://doi.org/10.1016/j.atmosres.2006.09.003>, 2007a.
- 1462 Zhang, M., Wang, S., Wu, F., Yuan, X., and Zhang, Y.: Chemical compositions of wet precipitation and
1463 anthropogenic influences at a developing urban site in southeastern China, *Atmospheric Res.*, 84, 311–
1464 322, <https://doi.org/10.1016/j.atmosres.2006.09.003>, 2007b.
- 1465